

2001

JOHNSON

SAND83-0030 • UC-70
Unlimited Release
Printed May 1987

Nevada Nuclear Waste Storage Investigations Project

**Unit Evaluation at Yucca Mountain,
Nevada Test Site: Near-Field Thermal
and Mechanical Calculations Using the
SANDIA-ADINA Code**

Roy L. Johnson, Stephen J. Bauer

Prepared by
Sandia National Laboratories
Albuquerque, New Mexico 87185 and Livermore, California 94550
for the United States Department of Energy
under Contract DE-AC04-76DP00789

"Prepared by Nevada Nuclear Waste Storage Investigations (NNWSI) Project participants as part of the Civilian Radioactive Waste Management Program (CRWM). The NNWSI Project is managed by the Waste Management Project Office (WMPO) of the U. S. Department of Energy, Nevada Operations Office (DOE/NV). NNWSI Project work is sponsored by the Office of Geologic Repositories (OGR) of the DOE Office of Civilian Radioactive Waste Management (OCRWM)."

Issued by Sandia National Laboratories, operated for the United States Department of Energy by Sandia Corporation.

NOTICE: This report was prepared as an account of work sponsored by an agency of the United States Government. Neither the United States Government nor any agency thereof, nor any of their employees, nor any of their contractors, subcontractors, or their employees, makes any warranty, express or implied, or assumes any legal liability or responsibility for the accuracy, completeness, or usefulness of any information, apparatus, product, or process disclosed, or represents that its use would not infringe privately owned rights. Reference herein to any specific commercial product, process, or service by trade name, trademark, manufacturer, or otherwise, does not necessarily constitute or imply its endorsement, recommendation, or favoring by the United States Government, any agency thereof or any of their contractors or subcontractors. The views and opinions expressed herein do not necessarily state or reflect those of the United States Government, any agency thereof or any of their contractors or subcontractors.

Printed in the United States of America
Available from
National Technical Information Service
U.S. Department of Commerce
5285 Port Royal Road
Springfield, VA 22161

NTIS price codes
Printed copy: A04
Microfiche copy: A01

SAND83-0030

NNWSI UNIT EVALUATION AT YUCCA MOUNTAIN, NEVADA TEST SITE:
NEAR FIELD THERMAL AND MECHANICAL CALCULATIONS
USING THE SANDIA-ADINA CODE

Roy L. Johnson and Stephen J. Bauer

Sandia National Laboratories
Albuquerque, NM 87185

ABSTRACT

The Nevada Nuclear Waste Storage Investigations (NNWSI) Project, managed by the Nevada Operations Office of the U.S. Department of Energy, is examining the feasibility of siting a repository for high-level nuclear wastes at Yucca Mountain on and adjacent to the Nevada Test Site. The work described herein was completed in 1983 to provide part of the technical basis for selecting a single target repository horizon upon which to concentrate future activities. Presented in this report are the results of a comparative study of two candidate horizons, the welded, devitrified Topopah Spring Member of the Paintbrush Tuff, and the nonwelded, zeolitized Tuffaceous Beds of Calico Hills. The mechanical and thermomechanical response these two horizons was assessed by conducting thermal and thermomechanical calculations using a two-dimensional room and pillar geometry of the vertical waste emplacement option using average and limit properties for each. A modified version of the computer code ADINA (SANDIA-ADINA) containing a material model for rock masses with ubiquitous jointing was used in the calculations. Results of the calculations are presented as the units' capacity for storage of nuclear waste and stability of the emplacement room and pillar due to excavation and long-term heating. A comparison is made with a similar underground opening geometry sited in Grouse Canyon Tuff, using properties obtained from G-Tunnel--a horizon of known excavation characteristics.

Long-term stability of the excavated rooms was predicted for all units, as determined by evaluating regions of predicted joint slip as the result of excavation and subsequent thermal loading, evaluating regions of predicted rock matrix failure as the result of excavation and subsequent thermal loading, and evaluating safety factors against rock matrix failure. These results were derived through considering a wide range in material properties and in situ stresses. It is prudent to further conclude that future calculations would predict stable openings if the material properties used, and in situ stresses fell within the ranges considered here.

CONTENTS

	<u>Page</u>
INTRODUCTION.	1
THERMAL ANALYSES.	3
General.	3
Finite Element Discretization.	3
Thermal Properties of Tuff	3
Thermal Properties of the Waste.	7
Radiation Approximation.	9
Equivalent Volumetric Heat Source.	9
Optimized Gross Thermal Loadings	9
Results of the Thermal Calculations.	11
THERMOMECHANICAL ANALYSES	18
General.	18
Mechanical Properties of Tuffs	18
Finite Element Analysis.	20
Failure Criteria	22
Safety Factor.	25
Results of the Thermomechanical Analyses	26
Topopah Spring.	26
Calico Hills.	31
Grouse Canyon	36
Discussion	42
SUMMARY AND CONCLUSIONS	44
REFERENCES.	47
APPENDIX I- RIB and SEPDB Data	49

FIGURES

<u>Figure</u>	<u>Title</u>	<u>Page</u>
1	Typical Finite Element Mesh Used in the Thermal Computations, with Enlarged Detail Shown in the Region of the Room	6
2	Typical Variation of Conductivity with Temperature, Assuming Boiling of Groundwater at 100°C	8
3	Typical Variation of Heat Capacity with Temperature, Assuming Boiling of Groundwater at 100°C.	8
4	Isotherms at Various Times after Emplacement of the Waste for Topopah Spring (Average Properties).	12
5	Isotherms at Various Times after Emplacement of the Waste for Calico Hills (Average Properties).	15
6	Typical Finite Element Mesh Used in the Thermo-mechanical Computations with Enlarged Detail Shown in the Region of the Room.	21
7	Joint Failure Criterion.	23
8	Rock Matrix Failure Criterion.	24
9	Regions of Joint Movement for Topopah Spring	27
10	Fractured Matrix Regions for Topopah Spring to 100 Years	28
11	Matrix Factor of Safety Contours for Topopah Spring at Various Times (Average Properties).	29
12	Matrix Factor of Safety Contours for Topopah Spring at Various Times (Limit Properties).	30
13	Regions of Joint Movement for Calico Hills.	32
14	Joint Movement at Various Times for Calico Hills (Limit Properties)	33
15	Cumulative Joint Movement in First 100 Years for Calico Hills (Limit Properties).	34
16	Fractured Matrix Regions for Calico Hills Due to Excavation and 100 Years of Heating.	35

<u>Figure</u>	<u>Title</u>	<u>Page</u>
17	Matrix Factor of Safety Contours for Calico Hills (Average Properties) at Various Times.	37
18	Matrix Factor of Safety Contours for Calico Hills (Limit Properties) at Various Times.	38
19	Predicted Fractured Matrix Regions for Calico Hills (Limit Properties) with Ubiquitous Joints Deleted. . .	39
20	Regions of Joint Movement for Grouse Canyon at Excavation	40
21	Comparison of Regions of Predicted Joint Movement at Excavation for All Horizons Including Grouse Canyon. .	41

TABLES

<u>Table</u>		<u>Page</u>
1	Relative Heat-Generation Decay Properties.	4
2	Average Case Thermal Properties of Tuff.	5
3	Limit Case Thermal Properties of Tuff.	5
4	Equivalent Volumetric Heat Sources	10
5	Average and Limit Case Mechanical Properties for All Horizons	19

INTRODUCTION

The Nevada Nuclear Waste Storage Investigations (NNWSI) Project, managed by the Nevada Operations Office of the U.S. Department of Energy, is examining the feasibility of siting a geologic repository for high-level nuclear wastes at Yucca Mountain, on and adjacent to the Nevada Test Site in southern Nevada. The work described herein was completed in 1983 and contributed to the technical basis for selection of a single target repository horizon upon which to concentrate future activities. As such, the decision or horizon choice considered these calculations including the material properties, boundary conditions, in situ conditions, and assumed material behavior reflects the NNWSI Project perspective of the subject for the 1981-1982 time frame. This work, and that of a companion report [1] serve to document the thermomechanical calculations used in the unit evaluation study [2].

Thermal and thermomechanical calculations were performed for four horizons that had been identified as potential candidates for a repository. They are the welded, devitrified Topopah Spring Member of the Paintbrush Tuff; the welded, devitrified portions of the Bullfrog and Tram Members of the Crater Flat Tuff; and the nonwelded, zeolitized Tuffaceous Beds of Calico Hills. After the calculations were completed, the Topopah Spring Member was selected as the potential target horizon. Consequently, selected thermal and thermomechanical calculations for the Topopah Spring Member are reported herein along with similar analyses for the Calico Hills unit for comparative purposes. The detailed results of thermal and thermomechanical calculations for the Topopah Spring, Bullfrog, Tram, and Calico Hills units were archived in the SNL/NNWSI Records File. Within the unit evaluation study the Calico Hills unit ranked the lowest. The results for the Calico Hills are presented here to demonstrate the predicted response for this low ranked, yet acceptable response; as a bounding type of behavior. The Topopah Spring and parts of the Tuffaceous Beds of Calico Hills are located in the unsaturated zone above the water table.

The calculations performed utilized the vertical emplacement mode geometry. The calculations were performed using average and limit properties for each of the candidate horizons [3-11]. At the time these calculations were performed, material properties were determined through empirical relationships which related the porosity to the desired set of material properties. Average material properties were determined for a unit by first

selecting the average porosity, and then calculating all the necessary material properties for the analysis. As such the values of all material properties for both average and limit cases are dependent on the porosity value chosen. An increase in porosity was used for the limit cases considered, and the material properties listed for each unit reflect the result of that increase in porosity. Limit properties were intended to provide a reasonable estimate of a bounding condition which might be encountered in any given horizon. Performance assessment based on the use of these properties might be expected to produce a "lower bound" on the predicted behavior of each horizon.

Performance of the two horizons was assessed on the basis of four different criteria: (1) radionuclide isolation time, (2) allowable repository gross thermal loading, (3) excavation stability during an extended period of heating for up to 100 years, and (4) relative economics. The first and fourth performance criteria are not the subject of this report and are discussed elsewhere [2]. The second criterion was based on a specified maximum temperature of 100°C at the floor of the room 110 years after emplacement. This criterion resulted from the potential need to retrieve the waste and the environment perceived necessary for human entry to accomplish retrieval. The maximum, gross thermal loadings (GTLs) were obtained from a series of thermal calculations for each horizon to find the GTL that would produce a maximum temperature at room floor centerline of 100°C after a 110-year period of heating. The horizons were then compared based on their respective maximum GTLs.

Performance criterion (3) was based on stability considerations using data obtained from mechanical (excavation) and thermomechanical (superposed thermally induced loads) calculations. The stability considerations included regions of predicted joint slip as a result of excavation and subsequent thermal loading, regions of predicted rock matrix failure as a result of excavation and subsequent thermal loading, and safety factors against rock matrix failure. A comparison based on this performance criterion was also done.

All thermal calculations were done using the 1978 version of the computer code ADINAT [12]. Thermomechanical calculations were performed using the computer code SANDIA-ADINA [13,14], a modified version of ADINA [15] that includes a material model for rock masses with ubiquitous jointing [13]. All computer plots were generated using the computer code DETOUR [16].

THERMAL ANALYSES

General

Four thermal calculations were performed, one for each of the two horizons, using average and limit values of the thermal properties. The GTL for each horizon was determined from a series of calculations to obtain a desired value as discussed in a later paragraph.

Relative heat generation decay rates used in the calculations for the 10-year-old spent-fuel (SF) waste are listed in Table 1.

Thermal material properties for the various units were assumed to be constant through the depth of the emplacement horizon. Boiling of the groundwater was assumed to occur at 100°C. Initial temperatures for each of the horizons are shown in Tables 2 and 3.

Finite Element Discretization

Figure 1 shows plots of the complete finite element thermal mesh and a portion of the mesh enlarged in the region of the room. Points A through E define the limits of the room excavation. The mesh extended 250 m above and below the floor of the room. Material properties were the same throughout the modeled region even though the distance of 250 m above and below the floor of the room crosses material property boundaries. This simplification in the analysis was considered appropriate based on the "comparative" purposes of the analyses. More recent thermal analyses currently under way show that the vertical variation in material properties produce only minor thermal effects near the room. This distance was sufficient to maintain the isothermal boundary condition at the upper and lower boundaries of the mesh for a period of 200 years after emplacement of the waste. A total of 100 time steps were used in the calculations for the period 0 to 110 years.

Thermal Properties of Tuffs

Average and limit values of thermal conductivity, K , and heat capacity, ρC_p , were specified for each candidate horizon as being representative values for these units at the time the calculations were performed [3-11]. These values are summarized in Tables 2 and 3.

Thermal conductivities are specified for the rock in the saturated and dry states and are assumed to vary linearly between these two values over a transition temperature range as shown in Figure 2. A spike in the heat

Table 1

Relative Heat-Generation Decay Properties^a

Year after Emplacement ^b	Normalized Power for Spent Fuel
0	1.0
1	.956
2	.919
3	.889
4	.861
5	.838
6	.819
7	.799
8	.782
9	.763
10	.750
15	.681
20	.622
30	.525
40	.449
50	.387
70	.301
100	.238
190	.137
290	.108
390	.0919
490	.0806
590	.0711
690	.0633
790	.0569
890	.0514
990	.0466
1990	.0247
5990	.0148
9990	.0114

^aSee Y/OWI/TM-34, "Nuclear Waste Projections and Source Term Data for FY 1977." The HLW decay rates correspond to waste arising from fuel which is a 3.1 mix of fresh UO₂ and MOX fuels.

^bAssumes waste is 10 years old at emplacement.

TABLE 2

AVERAGE CASE THERMAL PROPERTIES OF TUFF

Horizon	Initial Temperature °C	Transition Temperatures-°C		Thermal Conductivity γ J/yr-m-°C x 10 ⁷		Heat Capacity J/m -°C x 10 ⁶			Heat of Vaporization J/m ³ x 10 ⁸
		Lower	Upper	Saturated	Dry	Saturated	Transition	Dry	
Topopah Spring	26.	100.	125.	5.68	4.92	2.18	10.34	1.76	2.09
Calico Hills	30.	100.	150.	4.10	2.84	2.72	16.42	1.34	7.20
Grouse Canyon	18.	100.	125.	5.75	4.55	2.46	15.18	1.84	3.26

TABLE 3

LIMIT CASE THERMAL PROPERTIES OF TUFF

Horizon	Initial Temperature °C	Transition Temperatures-°C		Thermal Conductivity γ J/yr-m-°C x 10 ⁷		Heat Capacity J/m -°C x 10 ⁶			Heat of Vaporization J/m ³ x 10 ⁸
		Lower	Upper	Saturated	Dry	Saturated	Transition	Dry	
Topopah Spring	29.	100.	125.	5.27	4.42	2.22	13.10	1.67	2.80
Calico Hills	34.	100.	150.	3.94	2.43	2.80	18.60	1.21	8.28

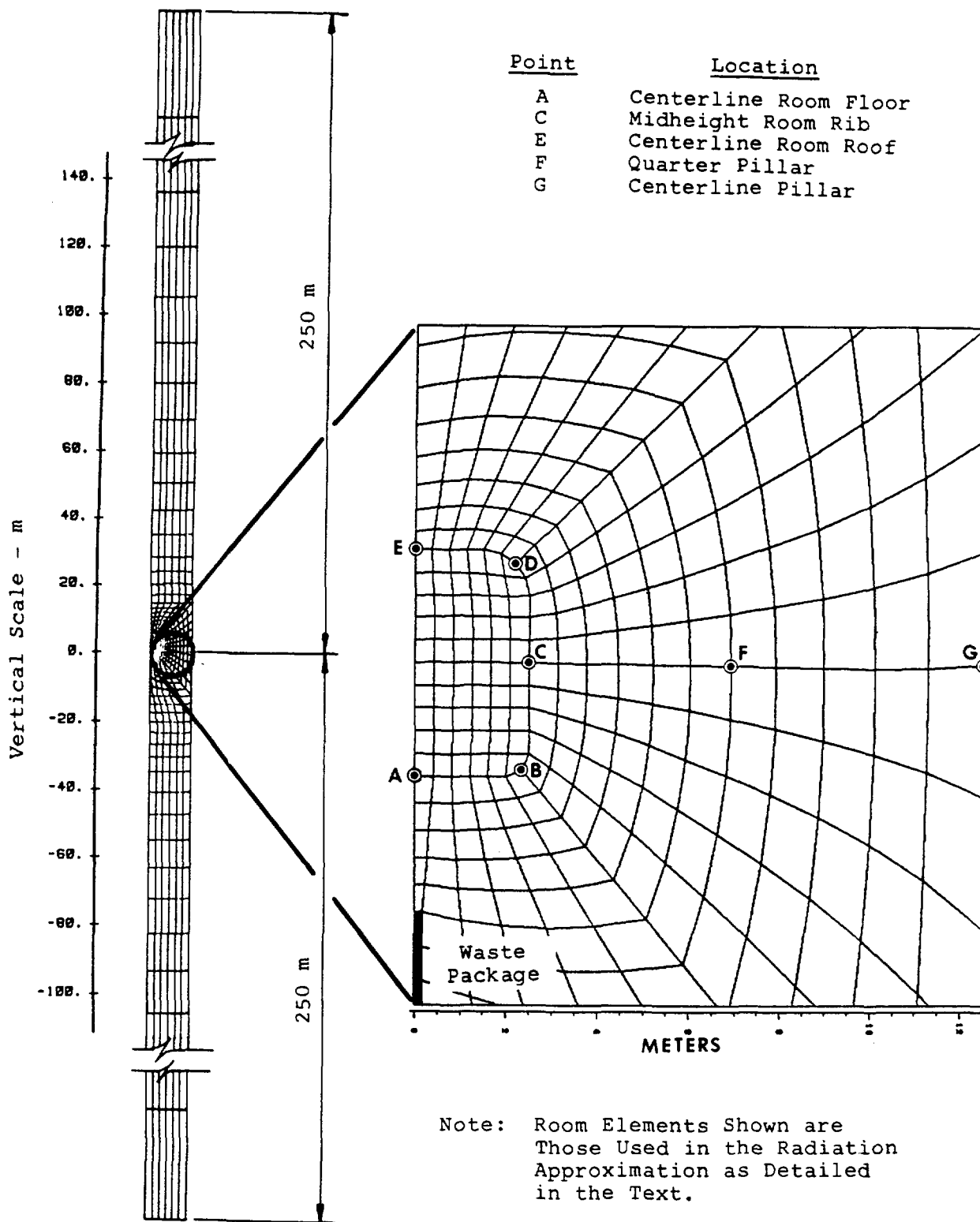


Figure 1. Typical Finite Element Mesh Used in the Thermal Computations with Enlarged Detail Shown in the Region of the Room.

capacities was introduced between the saturated and dry states to account for the latent heat of vaporization during boiling of the groundwater. The amplitude of the spike was computed by dividing the heat of vaporization by the difference between the upper and lower transition temperatures and adding this value to the average of the saturated and dry heat capacities. This variation in heat capacity is shown in Figure 3.

Thermal Properties of the Waste

The thermal properties of the elements representing the waste and canister were assumed constant over the temperature range considered, as follows:

$$K = 3.82 \times 10^7 \text{ J/yr-m-}^\circ\text{C}$$

$$\rho C_p = 2.51 \times 10^6 \text{ J/m}^3\text{-}^\circ\text{C}$$

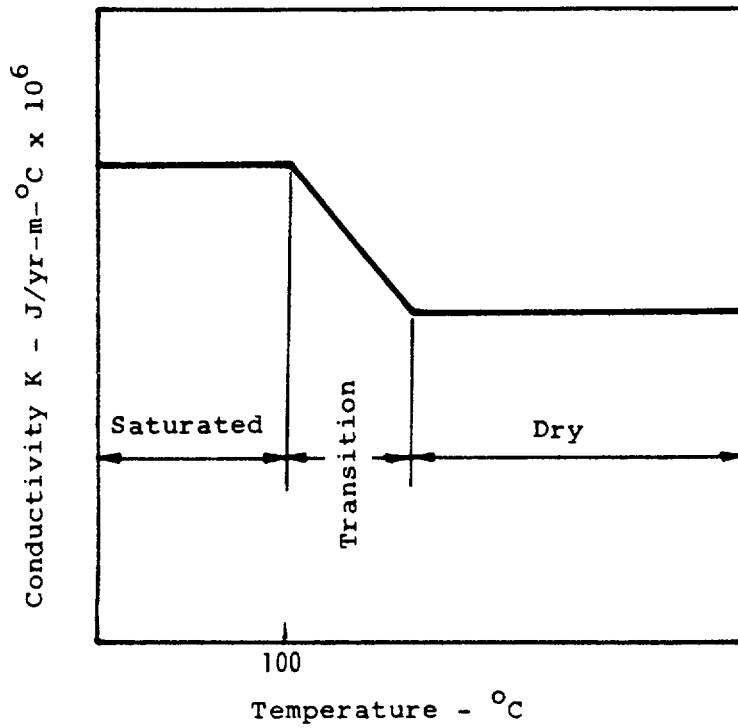


Figure 2. Typical Variation of Conductivity with Temperature Assuming Boiling of Groundwater at 100°C.

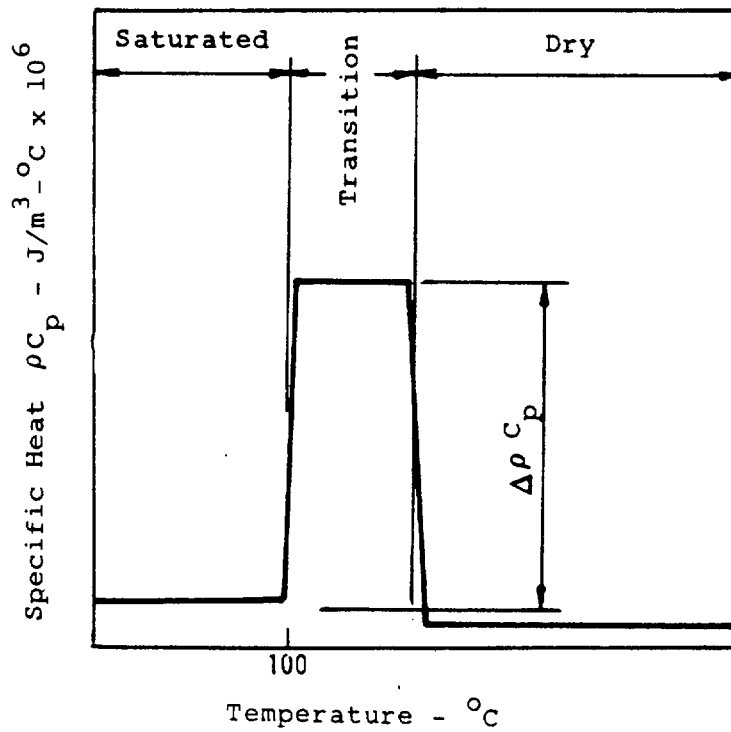


Figure 3. Typical Variation of Heat Capacity with Temperature Assuming Boiling of Groundwater at 100°C.

These properties correspond to those specified for commercial high level waste (CHLW) in previous reports [19,21]. The properties of spent fuel were previously assumed to be those of a temperature dependent composite of the UO_2 and canister. The motivation behind using the above properties was to choose a thermal conductivity sufficiently high that a rapid transfer of heat from the canister to the canister-rock mass interface was achieved. Differences in temperature distributions in the region of the room and pillar, away from the heat source, using the above properties rather than the actual properties, are expected to be negligible. Internal heat generation of the waste was computed on the basis of an equivalent volumetric heat source, as described in a later paragraph.

Radiation Approximation

The effects of radiation within the emplacement room, which was assumed to be air-filled and unventilated, were approximated by defining solid conduction elements with appropriate properties. The importance of thermal radiation in determining temperatures around the periphery of an air-filled room and that this radiation could be satisfactorily approximated by a thermal conduction model with a large diffusivity is shown in reference 19. In accordance with his recommendations, the following conduction properties were used here for modeling room elements:

$$K = 7.88 \times 10^8 \text{ J/yr-m-}^\circ\text{C}$$

$$\rho C_p = 1000 \text{ J/m}^3\text{-}^\circ\text{C}$$

Equivalent Volumetric Heat Source

The initial heat outputs, Q_o , used in these calculations are summarized in Table 4. These generation rates were calculated on the basis of an equivalent volume represented by a trench having the horizontal width and vertical height of the canister in the plane but extending continuously in the out-of-plane dimension. This equivalent heat source is a function of GTL or canister power, canister dimensions, and room-pillar width.

Optimized Gross Thermal Loadings

A GTL was computed for each horizon, based on the condition that a maximum temperature of 100°C be permitted at the

Table 4
Equivalent Volumetric Heat Sources

Horizon	Optimized GTL (kW/acre)	Q_0 (J/yr-M ³ x 10 ⁹)
Topopah Spring	56.9	6.844
Calico Hills	54.6	6.564

centerline of the room floor (point A) at 110 years after emplacement of the waste. Average case thermal properties were used for this series of calculations. The optimized GTL for each horizon is listed in Table 4 with the corresponding initial output of the canister expressed as an equivalent volumetric heat source.

Optimized GTLs were determined from a series of calculations in which the GTL for each horizon was adjusted so that the maximum temperature at floor centerline was not exceeded.

How groundwater boiling is treated in the thermal model approximates the real condition in the rock mass since it is assumed that the latent heat of vaporization is permanently removed from the system by evaporation and no recondensation is accounted for. At the time these calculations were made, no computer code was available to analyze water/vapor/air/energy transport. To assess the effects of these approximations, the GTL determination was repeated assuming that no boiling of the groundwater occurs. The assumption of no boiling would produce higher temperature differences above ambient than those calculated using the boiling condition; therefore, a GTL determined using this assumption would represent a lower bound on the thermal capacity of a given unit. Thermal properties for tuffs in the saturated condition were used for all horizons except the Topopah Spring, which was assumed to be 80% saturated. No significant change was found for the Topopah Spring. The Calico Hills showed a slightly smaller GTL when boiling was not considered, but the difference was minor. Apparently, the loss of heat capacity due to suppression of boiling is compensated for by a corresponding increase in conductivity, at least in the GTL range

considered. To verify this result, three additional calculations were made for Topopah Spring at GTLs of 30, 50 and 70 kW/acre. The resulting temperature rises above ambient at floor centerline were essentially linear with GTL up to approximately 50 kW/acre. At 70 kW/acre, the corresponding temperature rise for the no-boiling case was approximately 8 percent higher than that obtained using the assumption of boiling at 100°C.

Results of the Thermal Calculations

The determination of optimized GTLs as discussed above, was part of the results of the thermal calculations; and these GTLs are summarized in Table 4.

Nodal point temperatures computed using optimized GTLs and average and limit case thermal properties were used as input to the thermomechanical calculations described in the next section. Plots of isotherms obtained from these temperatures for the average case in the vicinity of the room and waste canister are shown in the Figures 4 and 5 for each of the horizons.

It will be noted that limit case temperatures at the floor centerline exceed 100°C. This is because the same GTLs determined using average case properties were used for both average and limit case thermal calculations.

The effects of groundwater boiling were found to be small, as indicated by the nearly linear variation of temperature rises for GTLs at or below 50 kW/acre. Only a few iterations were required to establish the optimum values shown in Table 4. This is probably because only a small region of the rock mass actually experienced temperatures above boiling.

For practical purposes, the calculated temperatures as a function of time and position in the Topopah Spring and Calico Hills are nearly identical and do not provide any means of discrimination. However, the optimized GTL for the Topopah Spring is slightly better (higher) than that of the Calico Hills. We can therefore attribute differences in the thermomechanical response presented in the following section to differences in the mechanical properties of the units considered.

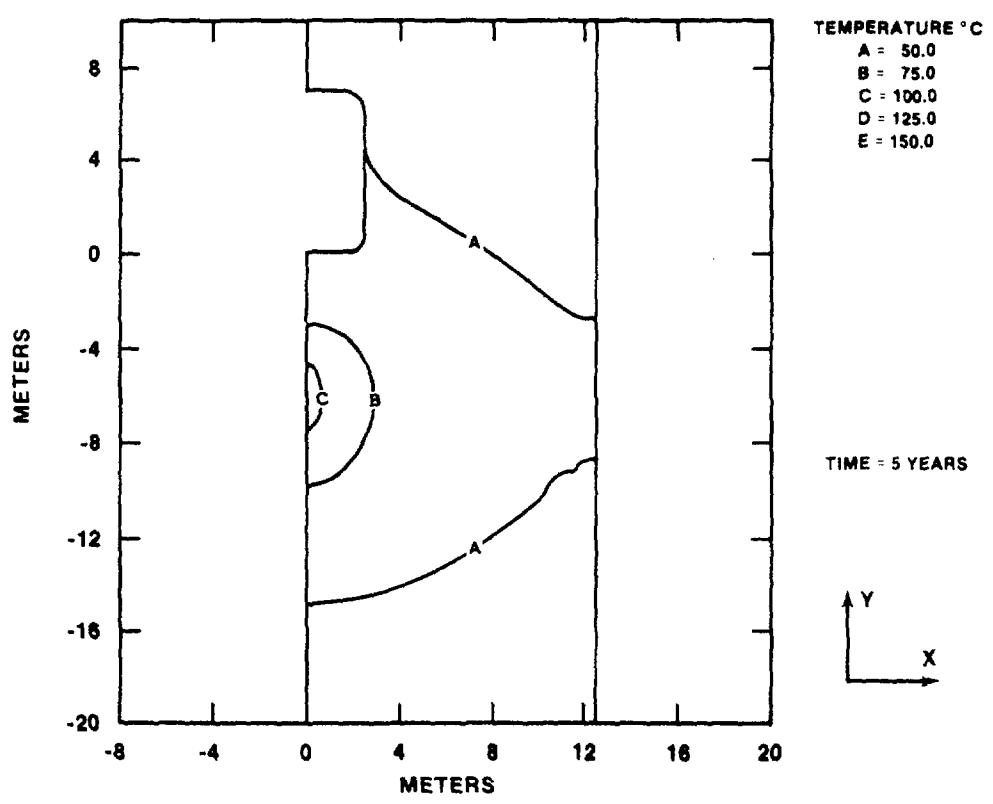
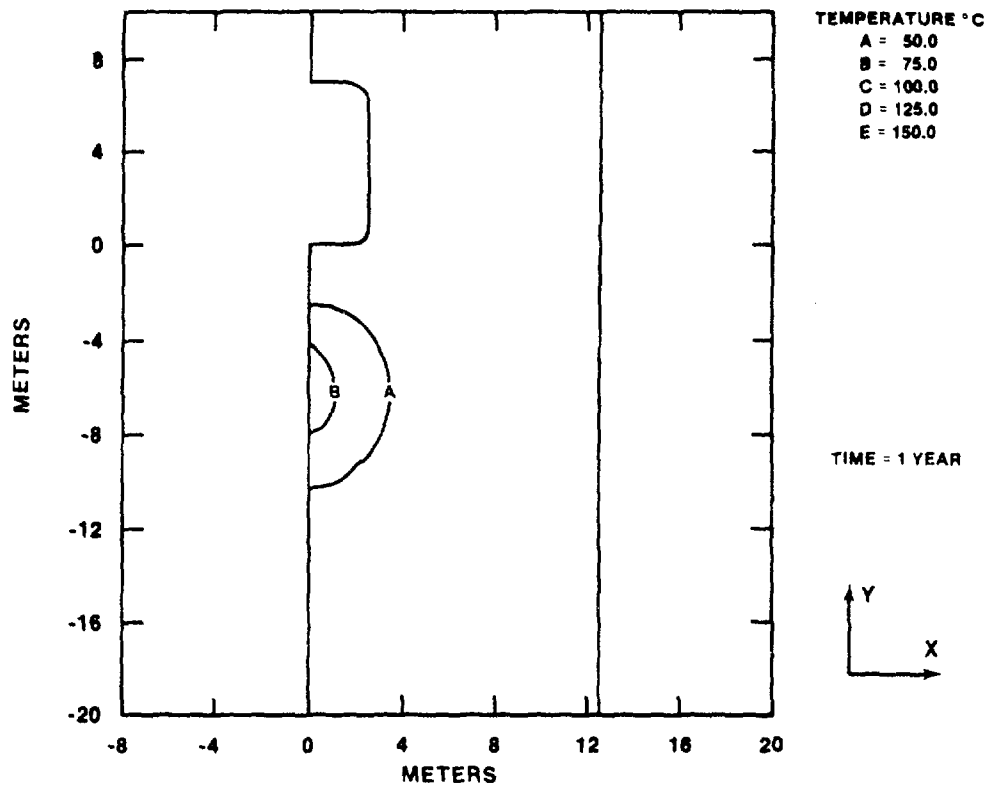


Figure 4. Isotherms at Various Times After Emplacement of the Waste for Topopah Spring (Average Properties).

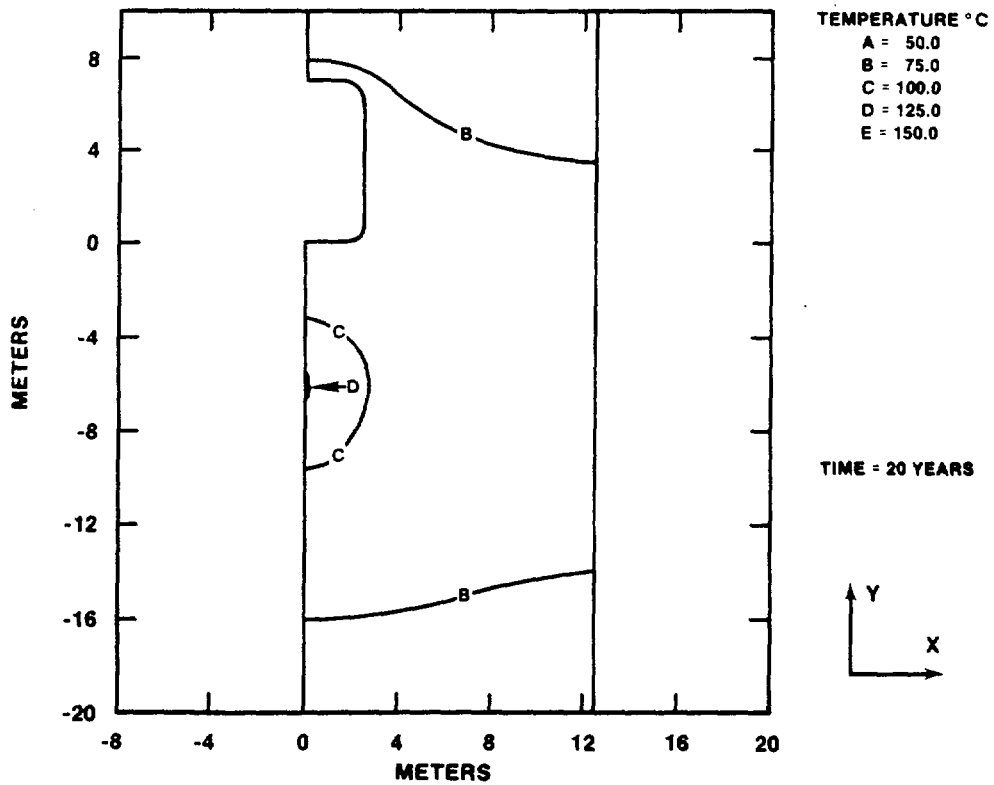
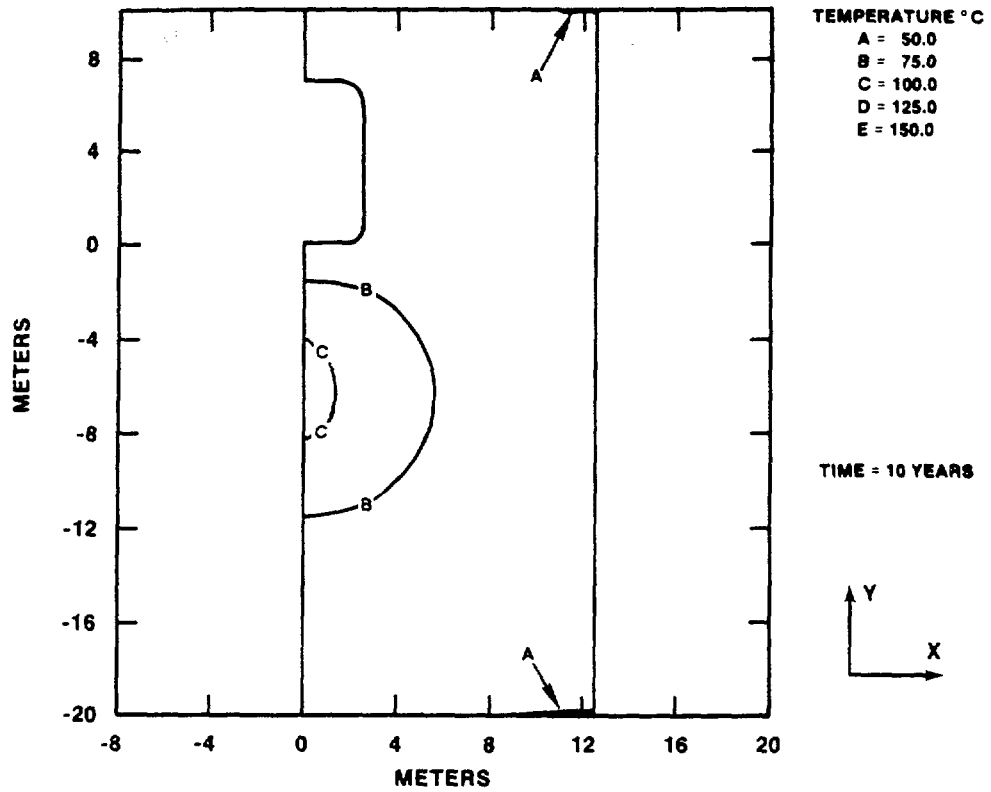


Figure 4. (Continued)

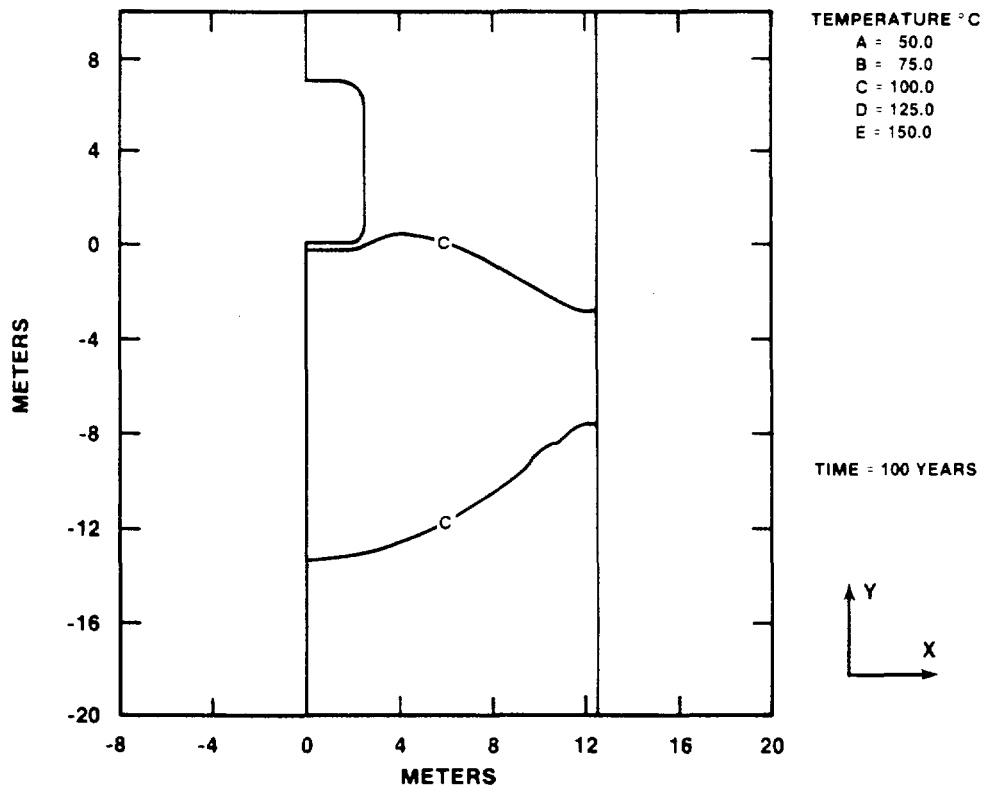
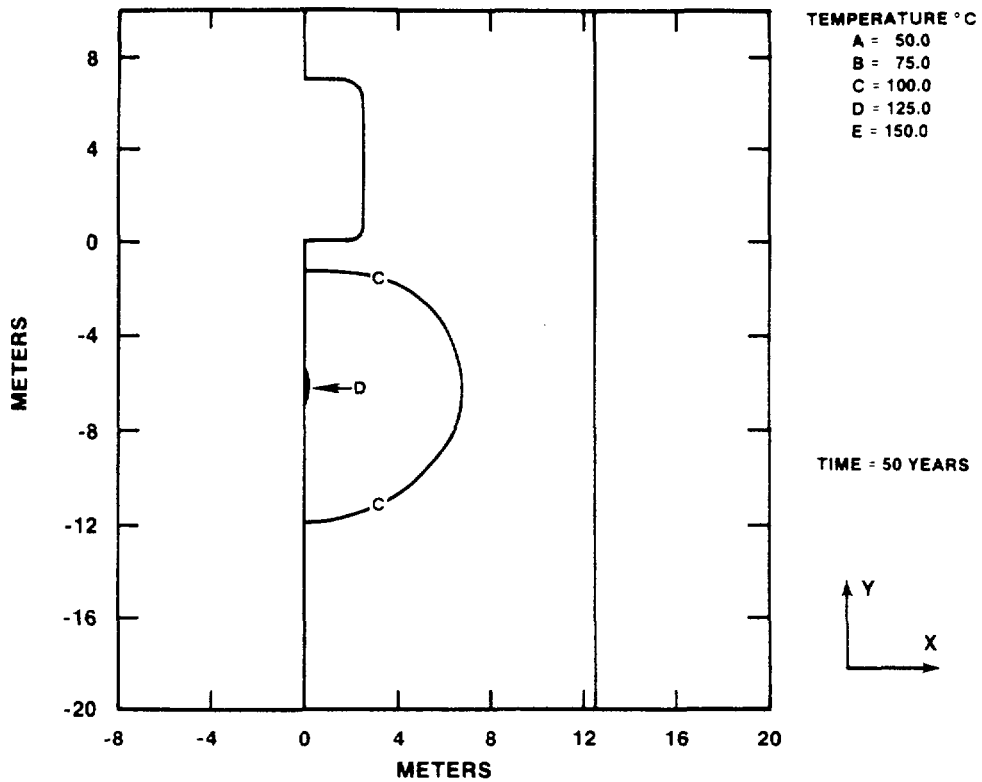


Figure 4. (Continued)

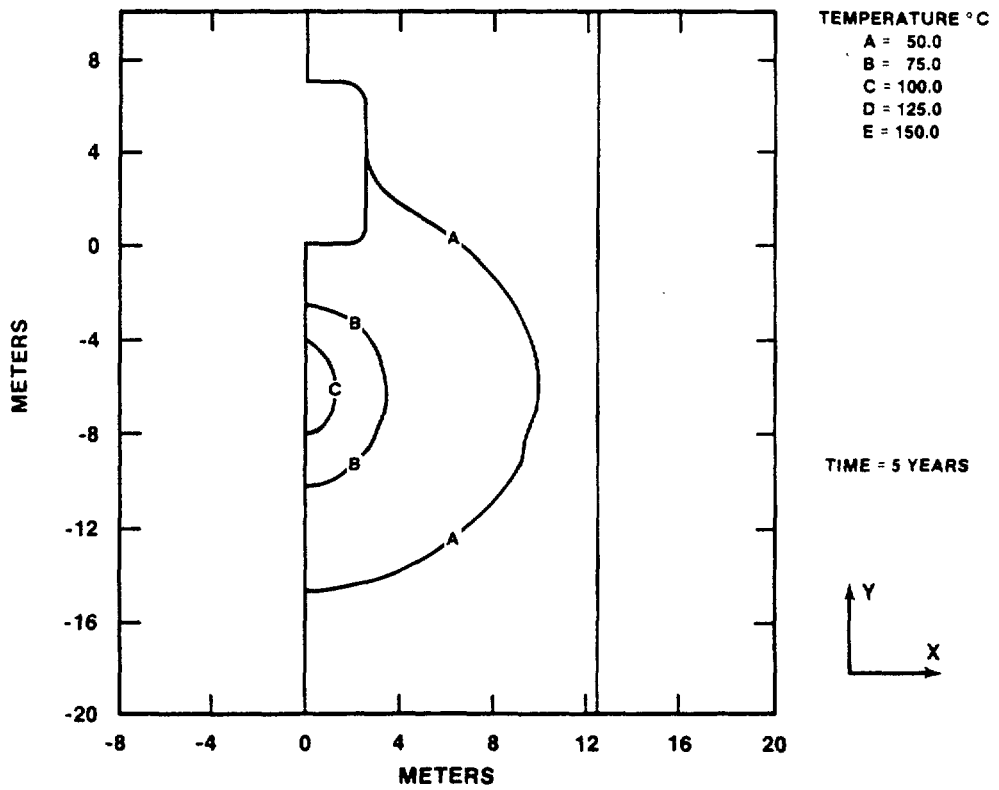
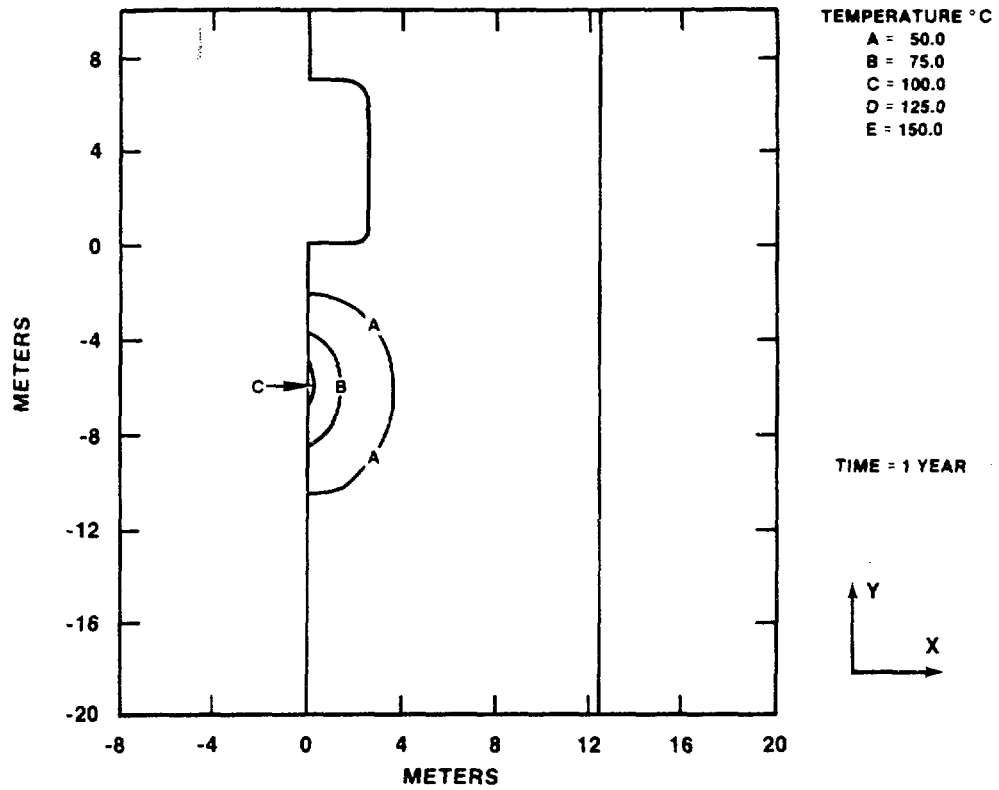


Figure 5. Isotherms at Various Times After Emplacement of the Waste for Calico Hills (Average Properties).

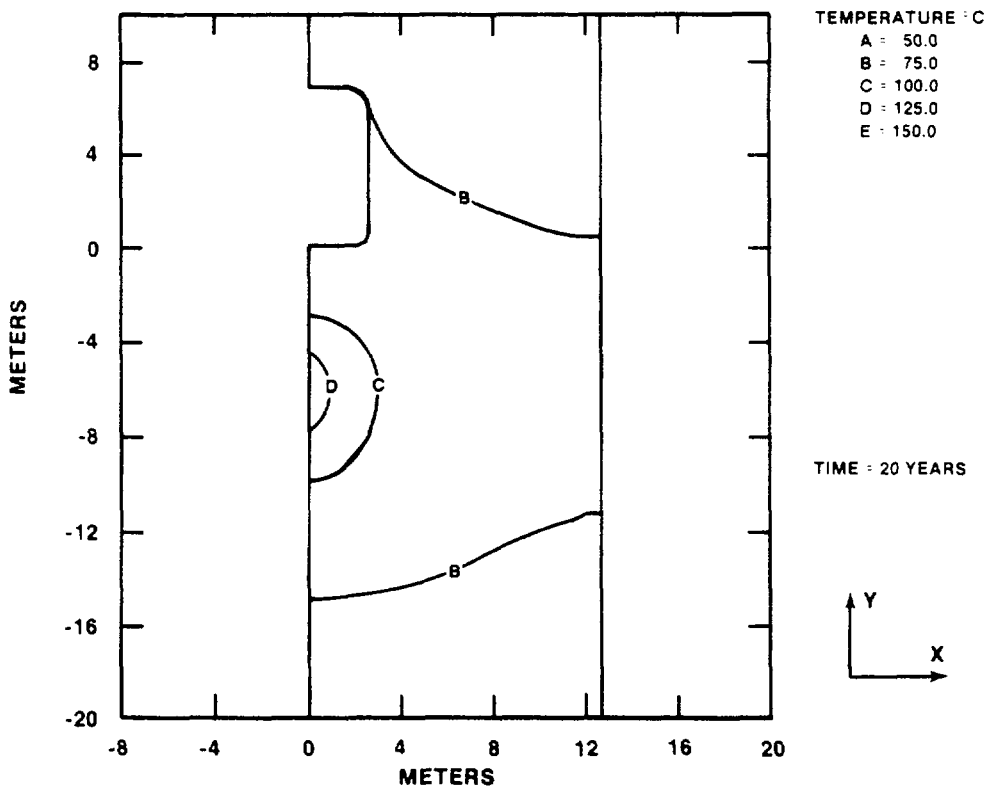
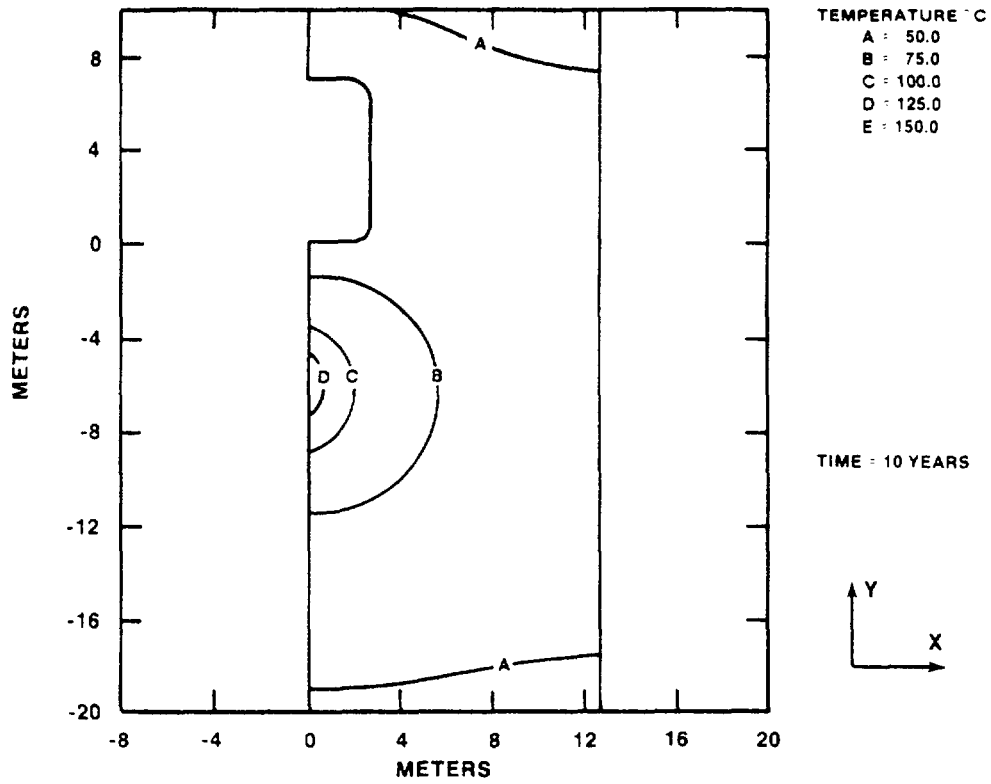


Figure 5. (Continued)

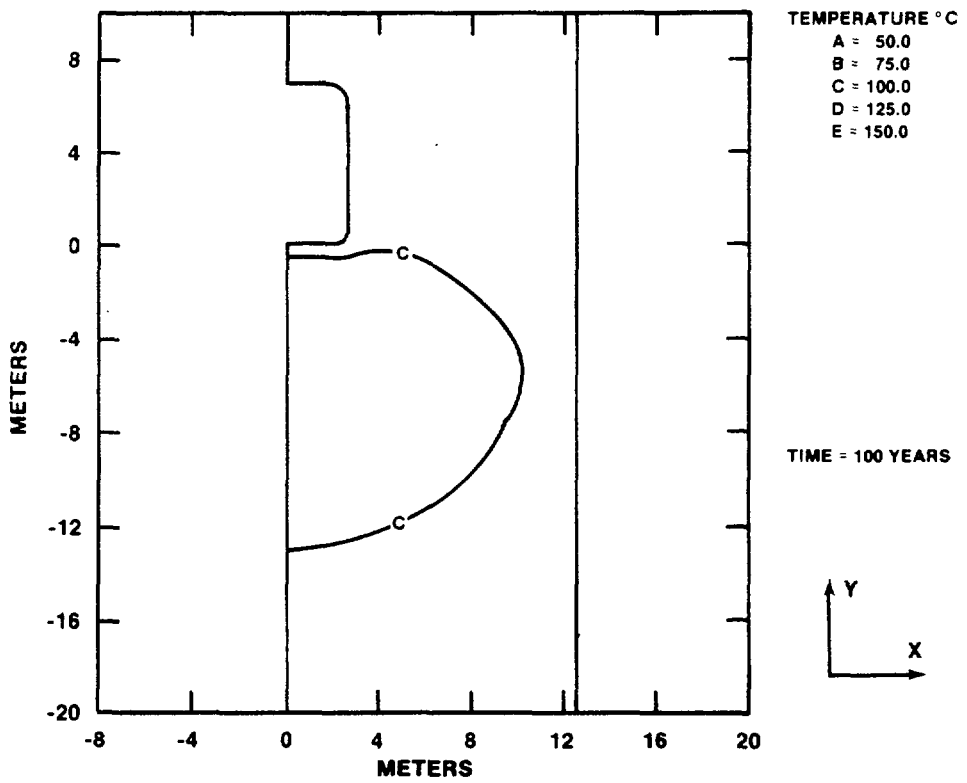
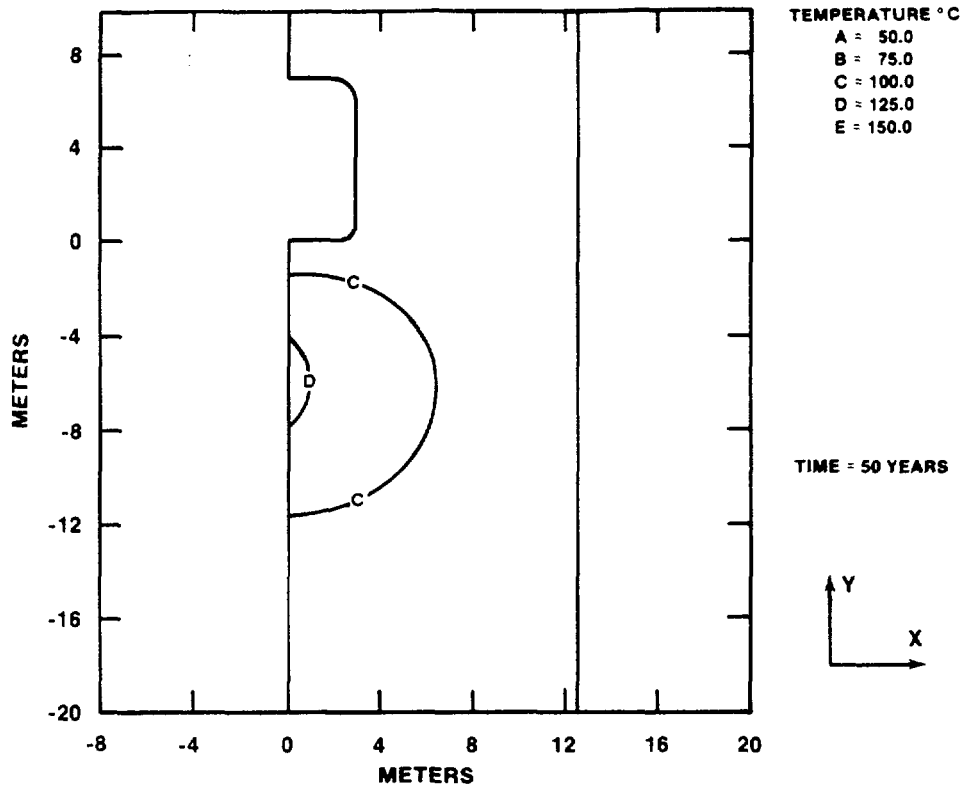


Figure 5. (Continued)

THERMOMECHANICAL ANALYSES

General

Calculations were performed for each candidate horizon, using average and limit values of mechanical properties. Comparison is made of the predicted behavior of the Topopah Spring and Calico Hills horizons with the observed behavior of excavations in the welded Grouse Canyon Member.

All analyses were performed using the finite element computer code ADINA [15], which was modified to include the jointed rock model presented in References 13 and 14.

Nodal point temperatures obtained from the thermal analyses using optimized GTLs for each horizon, were used as input to ADINA. Analyses were quasi-static and were performed for selected time steps. A total of 16 time steps were used to characterize the behavior of the room and pillar from the time of excavation to a time of 100 years after emplacement of the waste.

Mechanical Properties of Tuffs

Table 5 lists the values of the average and limit case mechanical properties used in the calculations. All properties were assumed to be independent of temperature except the coefficients of linear thermal expansion. These coefficients are specified over three temperature ranges, low (l), intermediate (m), and high (h). The applicable temperature ranges are indicated in parentheses below the corresponding expansion coefficients in Table 5. It should be noted that the Topopah Spring has a positive coefficient of thermal expansion for all temperature ranges, whereas in one case, the Calico Hills-Limit, the coefficient of thermal expansion is negative over all temperature ranges.

TABLE 5

Average and Limit Case Mechanical Properties

Property	Symbol	Unit	Horizon				Grouse ¹ Canyon
			Topopah Average	Spring Limit	Calico Hills Average	Limit	
Density	ρ		.00255	.00254	.00239	.00231	.00260
Young's Modulus	E	MPa	26,700.	18,200.	8100.	6300.	32,000.
Poisson's Ratio	ν	-	.14	.16	.16	.14	.13
Thermal Expansion Coefficient	$\alpha/l(\text{range})$	1/°C	10.7 (32-200)	14.1	6.7 (32-100)	-.40	6.2
	$\alpha_m/(\text{range})$	1/°C	31.8 (200-350)	53.6	-56.0 (100-150)	-115.0	--
	$\alpha_h/(\text{range})$	1/°C	15.5 (350-)	23.1	-4.5 (150-)	-9.3	8.9
Internal Friction Coefficient	μ_i	-	.488	.433	.279	.218	.554
Cohesion	C_o	MPa	28.5	20.7	10.9	9.0	16.2
Tension Cutoff	σ_c	MPa	12.8	9.4	0.1	0.1	4.0
Joint Friction Coefficient	μ_j	-	.800	.800	.550	.550	.800
Cohesion	C_o^j	MPa	1.0	0.0	0.4	0.0	1.0
Tension Cutoff	σ_c	MPa	0.1	0.1	0.1	0.1	0.1
Joint Angle	β	degrees	90.	90.	90.	90.	90.
In Situ Stresses	σ_y	MPa	-8.26	-10.85	-8.96	-13.40	-3.0
	σ_z	MPa	-8.60	-11.30	-10.30	-15.40	-8.1
	σ_x	MPa	-8.26	-10.85	-8.96	-13.40	-3.0
Quadratic Failure Surface Coefficient	S_{2j}	-	.0025	.0023	.0020	.0019	0.0

¹Average Properties Specified Only

Finite Element Analysis

Figure 6 shows a plot of the complete finite element mesh used in all of the thermomechanical calculations. A region of the mesh in the vicinity of the room has been enlarged to show details. Points around the periphery of the room and through the pillar are identified as points A through G.

Eight node quadrilateral elements integrated by 2 by 2 Gauss quadrature were used in the analyses. Since different meshes were used for the thermal and thermomechanical calculations, the computer program MERLIN [20] was used to interpolate nodal point temperatures between the two meshes. As mentioned before, 16 time steps were used in the analyses. These were selected from the 100 time steps used in the thermal analyses, and corresponding nodal point temperatures were used in the thermomechanical calculations.

To initialize stresses and simulate excavation, the first time step in the calculations was done with one set of rock mass properties specified throughout the modeled region. As such, elements were defined inside the room that had the same properties as the surrounding tuff. In the second time step, these elements were removed using the element death option in ADINA. Initial displacements and strains computed for the first time step were used to start the incremental solution; initial stresses in each element were set equal to the in situ stresses and nodal point temperatures set equal to initial temperatures. Thermal loads were applied after excavation, as determined from the thermal analyses.

Opening and closing of the joints, slip along joint planes, and intact rock failure were governed by failure criteria discussed in the following paragraph. Initially, all joints were assumed to be closed.

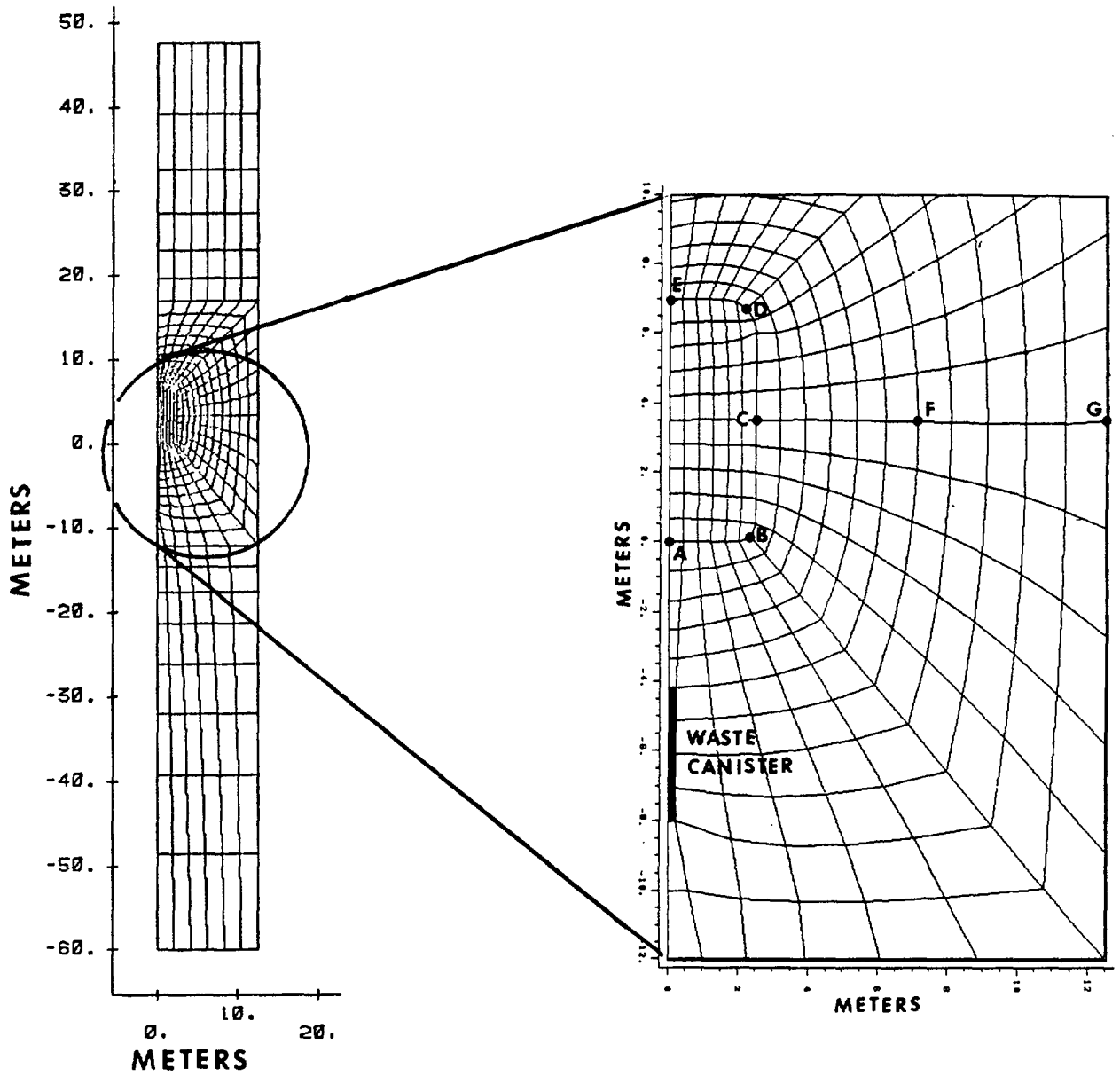


Figure 6. Typical Finite Element Mesh Used in the Thermo-Mechanical Computations with Enlarged Detail Shown in the Region of the Room.

Failure Criteria

Failure criteria are presented in this report to denote two physical phenomena which the material model attempts to represent, slip along existing joint planes, and the creation of new fractures given sufficient deviatoric stress. The concept of failure is not meant to mean unsuable.

Slip along an existing joint plane is governed by a Coulomb-type failure surface, as shown in Figure 7. Strength parameters are the joint friction coefficient, μ_j , the joint cohesion, C_o^j , the joint tensile strength, σ_t^j , and S_{2j} , a quadratic coefficient necessary to ensure that the joint shear strength does not exceed the matrix strength.

If, at any step in the computations

$$|\tau| \geq C_o^j - \mu_j \sigma_{nn} - S_{2j} \sigma_{nn}^2 \quad ,$$

where σ_{nn} is the stress (compression negative) normal to the joint plane, then slip occurs and the stiffness matrix is modified and the computation proceeds as discussed in Reference 12.

Matrix failure is governed by a Drucker-Prager failure surface as shown in Figure 8. In this criterion, the parameters are the intact rock internal friction coefficient, μ_i ; the matrix cohesion, C_o^i , and the matrix tensile strength, σ_t^i . An additional parameter is the transition stress, σ_{tran} [13]. The value of the normal stress σ_{tran} governs the mode of failure, either splitting along lines of principal compression, or shearing along two planes, making equal angles with the direction of principal compression, as shown in Figure 8. This transition stress was assumed constant for all units (33.5 MPa) and its value was established by experimental observation of the failure mode occurring in triaxial tests (W. Ollson, personal communication).

Matrix failure is predicted when the Mohr's circle representing the computed state of stress becomes tangent to the failure surface. New slip planes resulting from matrix failure are introduced at finite element integration points where the criterion has been exceeded. Slip along these new planes is then governed by the joint failure criterion discussed above.

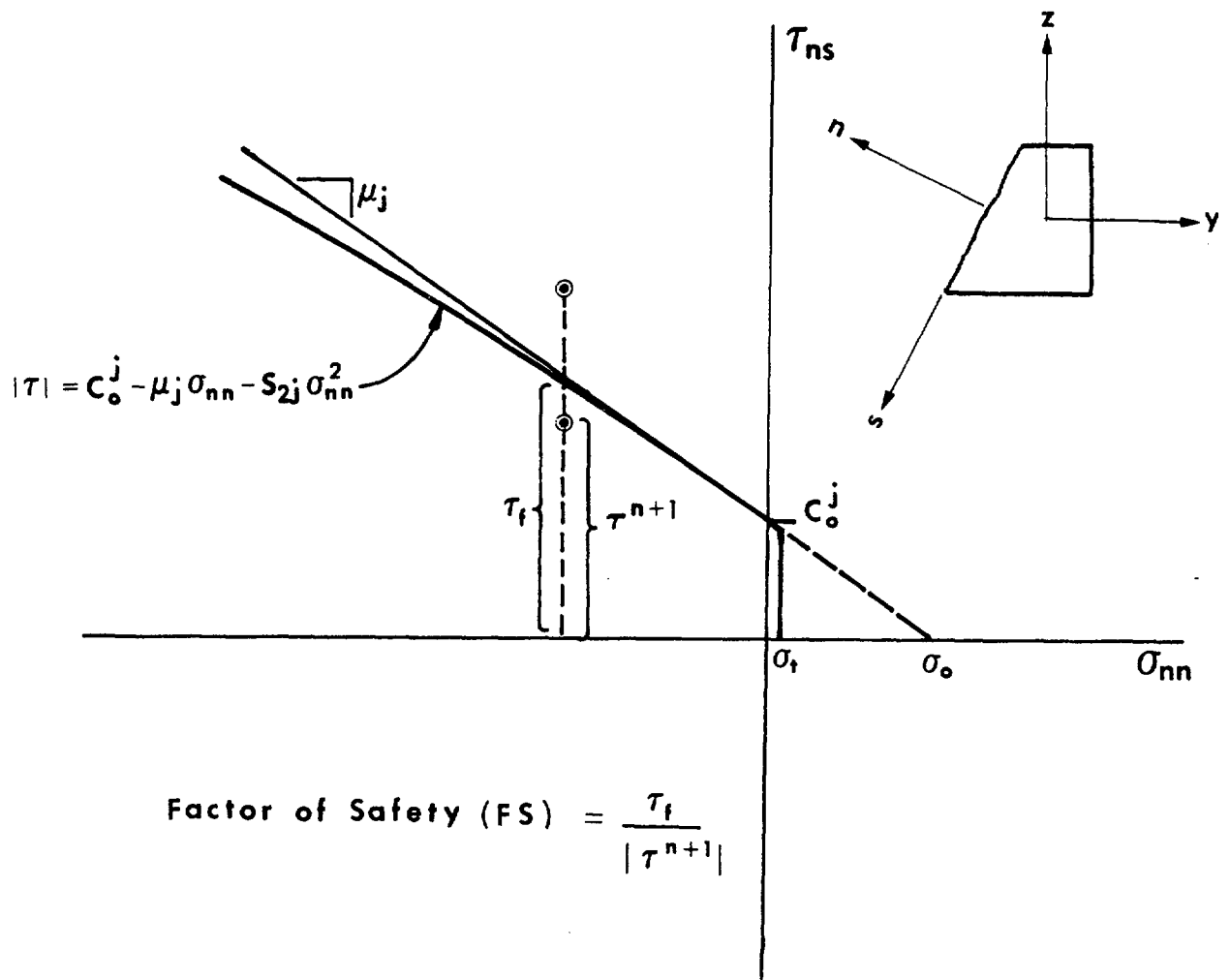


Figure 7. Joint Failure Criterion

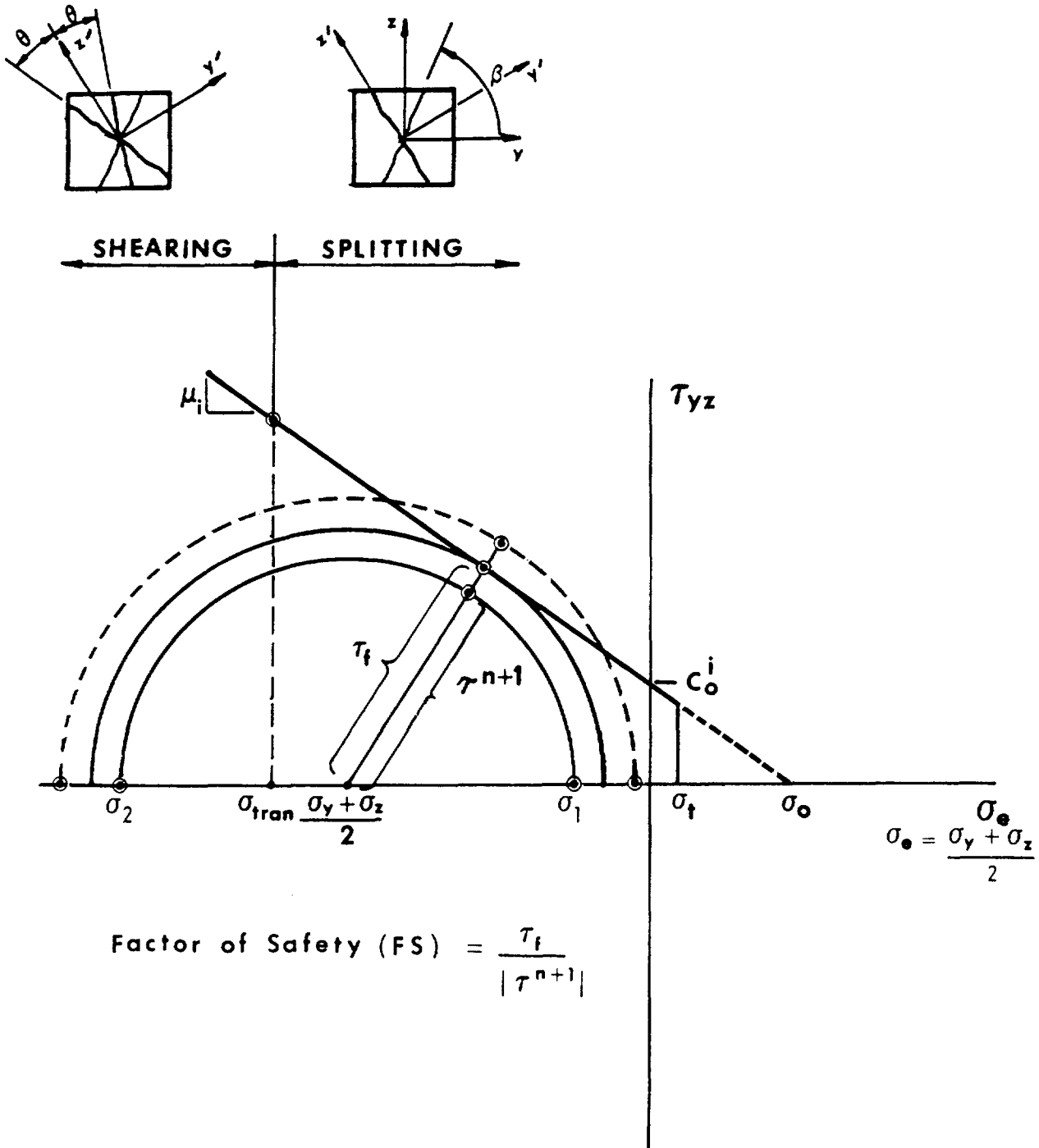


Figure 8. Rock Matrix Failure Criterion

Safety Factor

A safety factor is defined as the measure of strength divided by the measure of current stress.

For joints the shear strength, τ_f , is given by

$$\tau_f = |\tau| = C_o^j - \mu_j \sigma_{nn} - S_{2j} \sigma_{nn}^2$$

as shown in Figure 7. The current stress state, τ^{n+1} , is also shown in this figure. The safety factor against slip is then

$$\text{s.f.} = \frac{f}{|\tau^{n+1}|}$$

where in Figure 7 the safety factor is a number greater than 1 or less than 1 depending on whether the shear stress τ^{n+1} falls inside or outside the failure surface as shown.

The safety factor against matrix failure is of the same form as that used for joint slip. In Figure 8, τ_f is the radius of the Mohr's circle drawn tangent to the failure surface at a given confining pressure. The Mohr's circle representing the current state of stress, τ^{n+1} , may or may not intersect the failure surface shown in Figure 8. The safety factor is again given by

$$\text{s.f.} = \frac{\tau_f}{|\tau^{n+1}|} = \left[C_o^i + \mu_i \frac{(\sigma_1 + \sigma_2)}{2} \right] / \left| \frac{(\sigma_1 - \sigma_2)}{2} \right|$$

where σ_1 and σ_2 are the maximum and minimum principal stresses, respectively. A value of the safety factor greater than 1 indicates no predicted failure of the rock matrix. A no tension cutoff is an integral part of the material model.

In the computations, the potential for matrix failure, measured by the reciprocal of the safety factor against intact rock failure, is compared with the corresponding potential for joint slip. The mechanism having the larger potential is allowed to occur first.

Results of the Thermomechanical Analyses

Plots summarizing the results of the thermomechanical calculations for the Topopah Spring, Calico Hills, and Grouse Canyon units are shown in Figures 9 through 21. Typically, these are plots of (1) zones of joint movement due to excavation of the room and cumulative movement of the joints to 100 years after emplacement of the waste (heating) (2) zones of cumulative rock matrix failure after excavation and 100 years of heating, and (3) factors of safety against rock matrix failure at selected times.

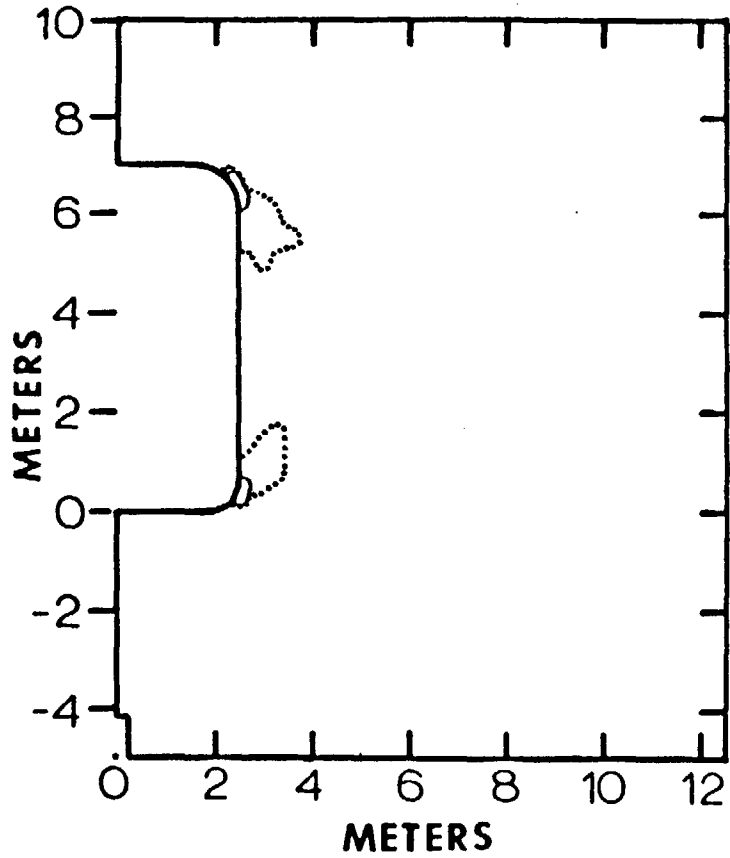
Of interest in the results of these calculations was the predicted stability of the room as a result of excavation and thermal loading after emplacement of the waste. All horizons were assumed to have a single, vertical joint set along which movement was monitored. A second joint set is created after matrix failure, as discussed above, and subsequent movement of this new joint set is also monitored. Lines defining the zones of joint movement and matrix failure are the envelopes of points at which joint movement or matrix failure has occurred at any time up to the time represented. The procedure is demonstrated later using the results of the Calico Hills calculations.

In what follows, the behavior of each horizon is discussed in separate paragraphs with a summary paragraph devoted to comparison of behavior of all horizons.

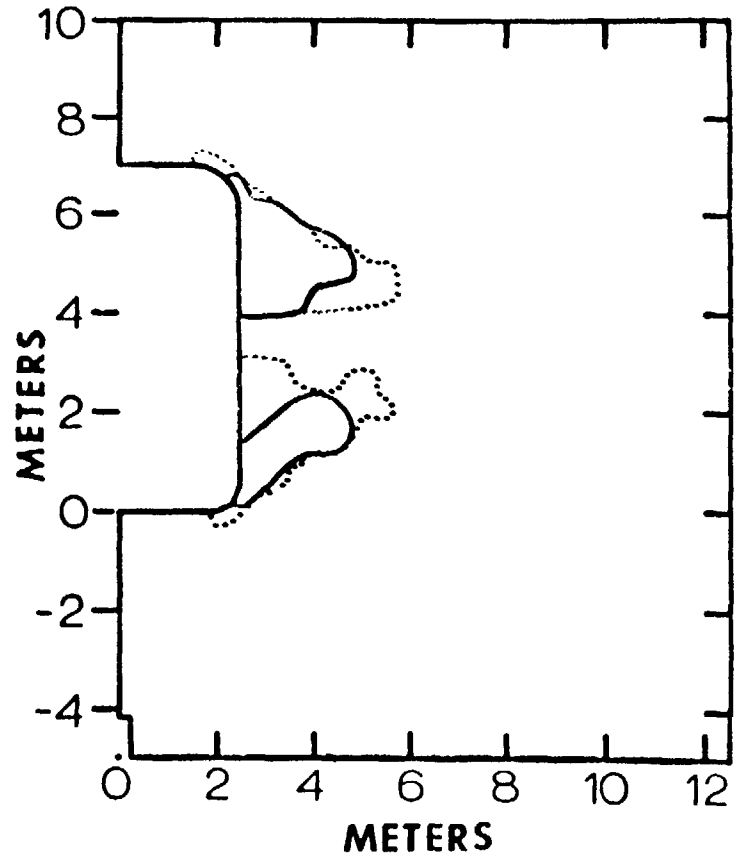
Topopah Spring

Figure 9a shows zones of joint movement at excavation for average and limit case mechanical properties. Zones of cumulative joint movement to 100 years after emplacement of the waste are shown in Figure 9b. Zones of cumulative matrix failure to 100 years after emplacement for limit case properties are shown in Figure 10. Matrix failure was first observed at 50 years. No matrix failures were predicted at any time using average case properties, and for limit case properties, matrix failure was predicted only in small regions near the corners of the room.

Contours of safety factors against matrix failure are shown for excavation and at 50 and 100 years after emplacement in Figure 11 for average case properties and in Figure 12 for limit case properties. Safety factors at excavation range from approximately 4.5 to > 9 for average case properties and 3 to > 9 for limit case properties.



a. At Excavation



b. Cumulative to 100 Years

Figure 9. Regions of Joint Movement for Topopah Spring. Solid Line - Average Properties; Dotted Line - Limit Properties.

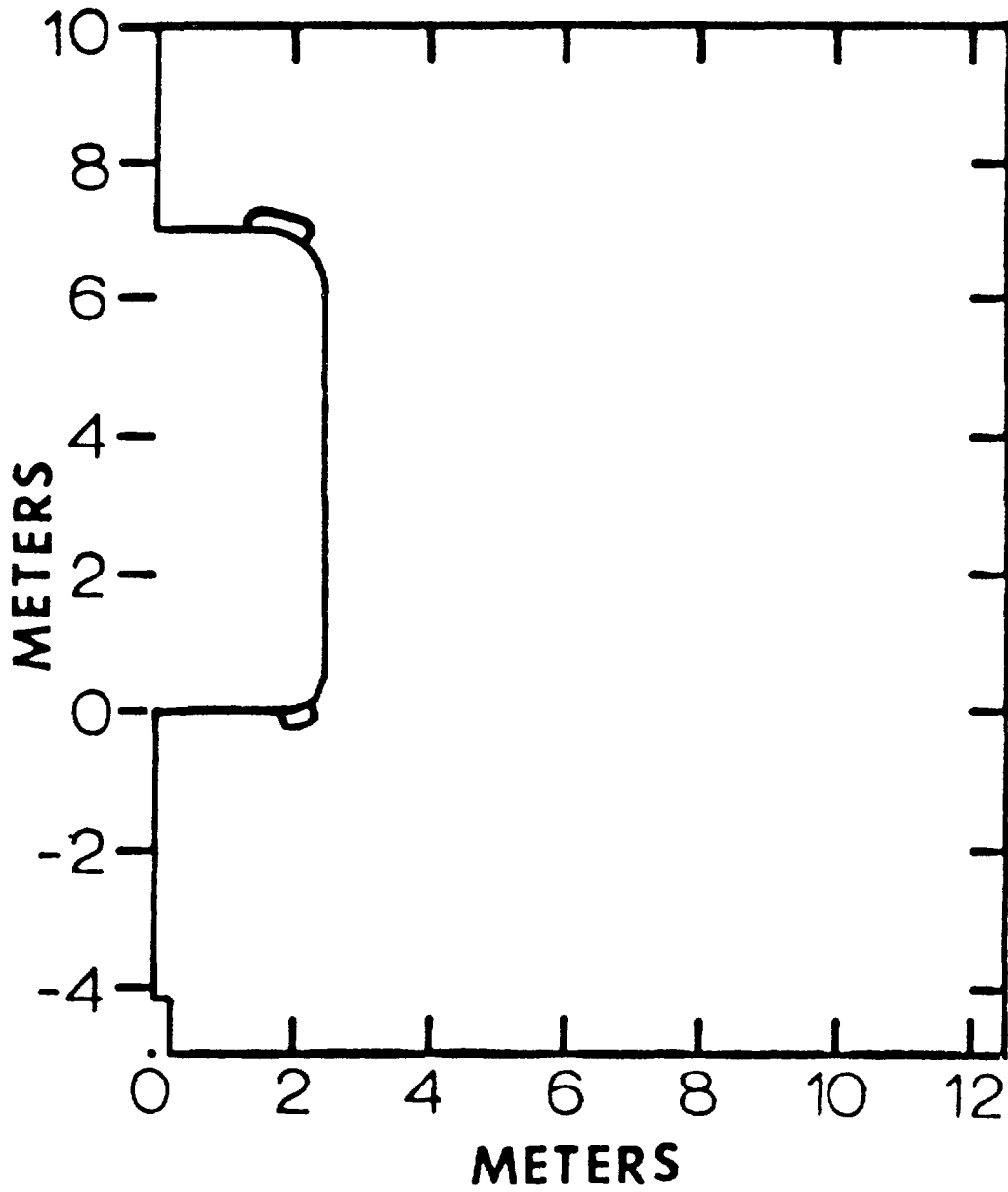


Figure 10. Fractured Matrix Regions for Topopah Spring to 100 Years. Limit Properties Shown (None for Average Properties).

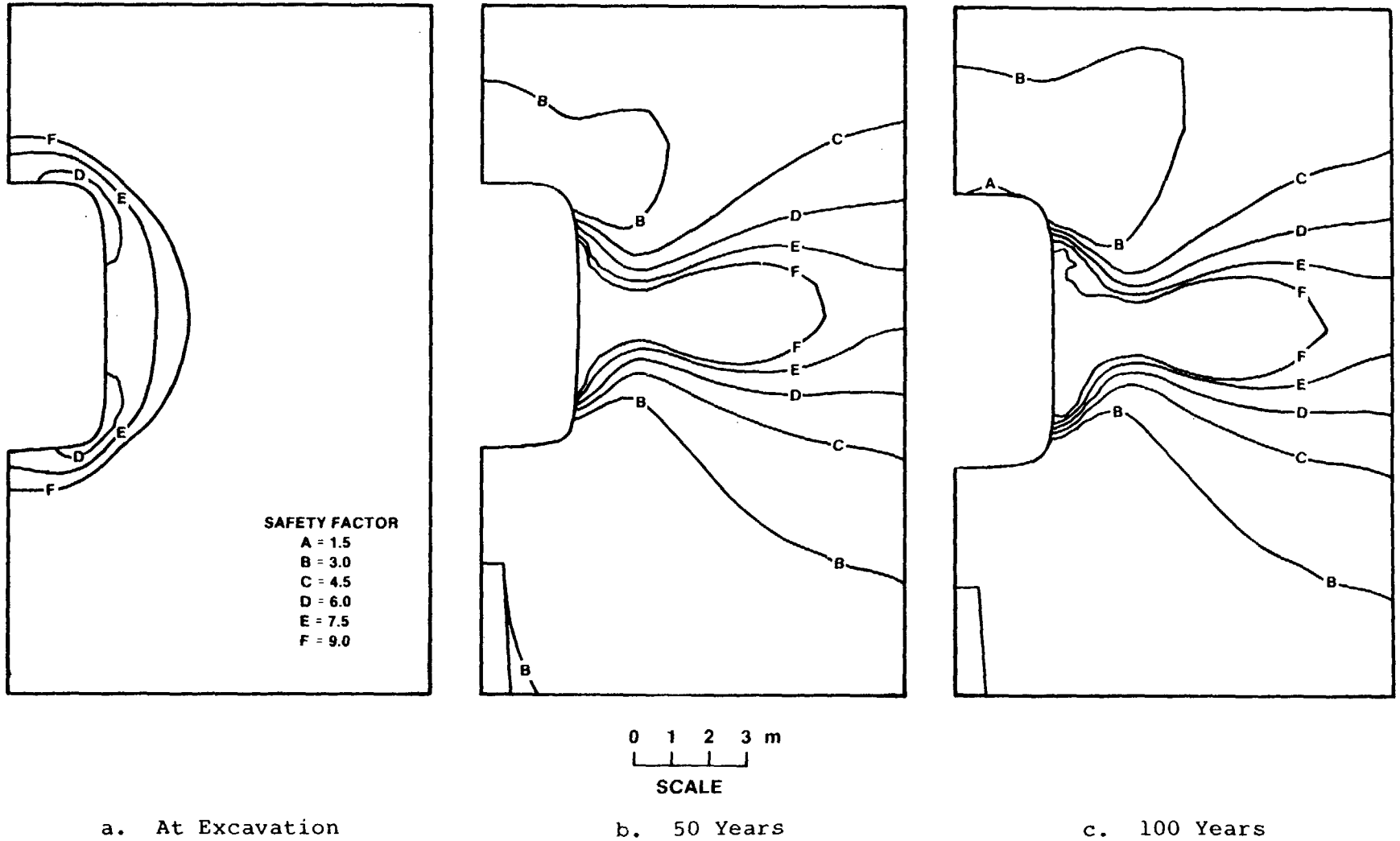


Figure 11. Matrix Factor of Safety Contours for Topopah Spring at Various Times (Average Properties).

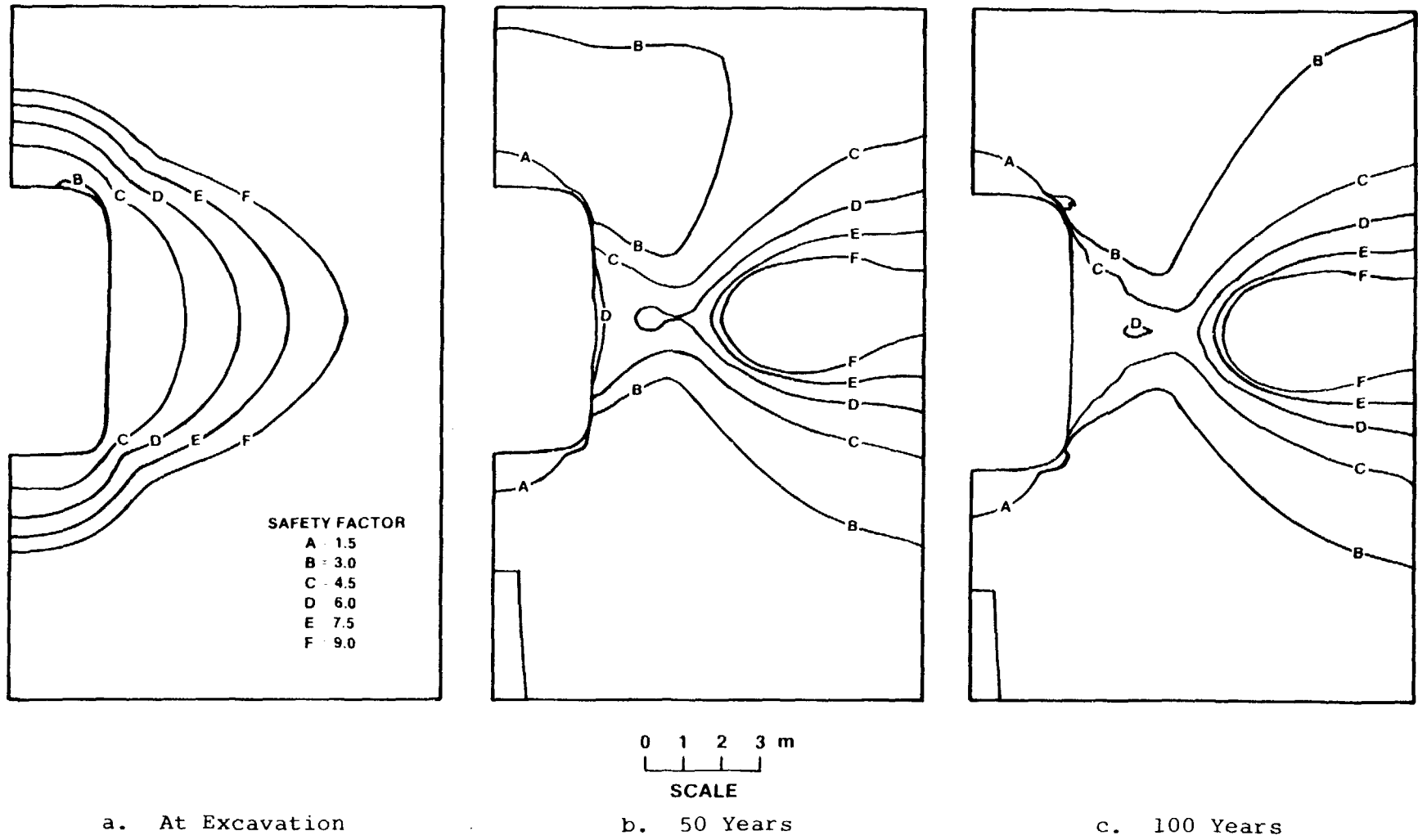


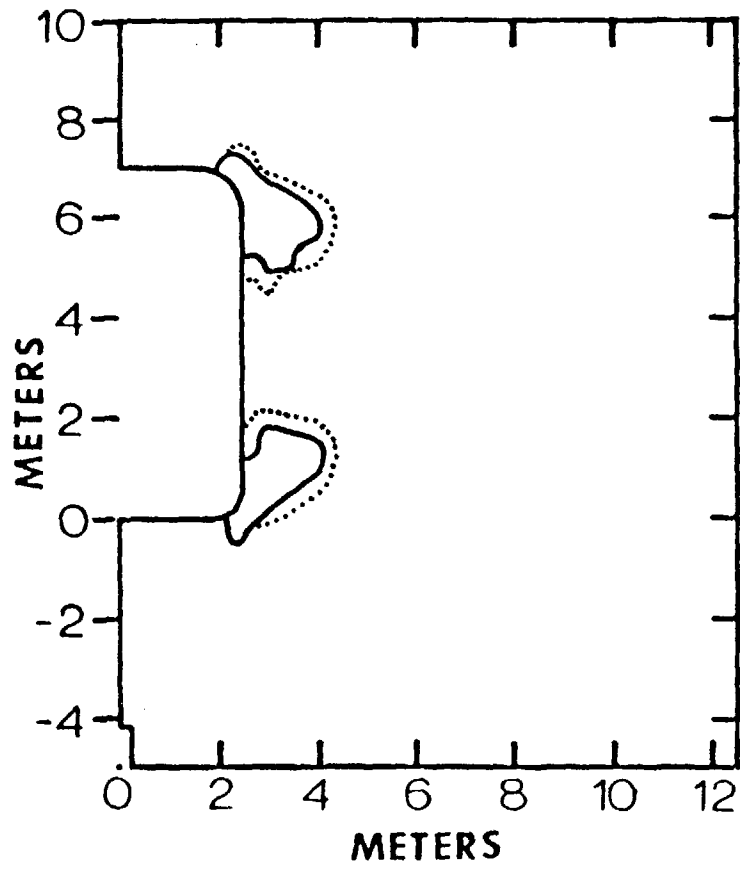
Figure 12. Matrix Factor of Safety Contours for Topopah Spring at Various Times (Limit Properties)

Calico Hills

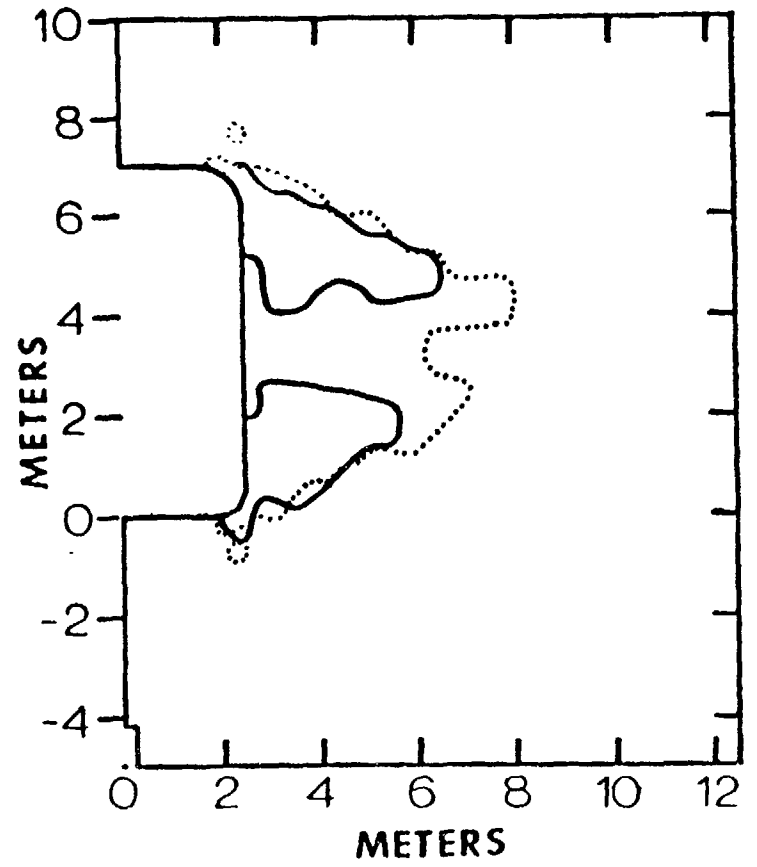
Figure 13a shows regions of joint movement due to excavation for both average and limit case properties. Regions of joint movement after 100 years of heating for both sets of properties are shown in Figure 13b. Figures 14 and 15 will be used to demonstrate how these zones were determined. Figure 14 is the computer-generated plot of joint movement at excavation and at the 50-year and 100-year time steps, respectively, using limit case properties. The cumulative plot of joint movement in Figure 15 includes all time steps to 100 years after emplacement. A solid "0" in this plot indicates that a joint has experienced both opening and slip during the 100-year time interval. The region of joint movement was determined by drawing a line enclosing all points exhibiting movement at any time up to the time represented, in other words, enclosing all points in the cumulative plots where joint movement has occurred at any previous time as shown by the dotted line in Figure 13b. A similar procedure was used to establish zones of matrix failure.

Note that in Figure 14, at the 100-year time step, the penetration of the zone of joint slippage extends slightly farther into the pillar, but more importantly, at 100 years, more of the joints are open. Joint opening results in a complete loss of shear resistance to slip on the plane of the joint, according to the assumed material behavior.

Rock matrix behavior after excavation is illustrated in Figure 16a for average material properties and in Figure 16b for limit properties. Using average material properties, no matrix failure was predicted at excavation.



a. At Excavation



b. Cumulative to 100 Years

Figure 13. Regions of Joint Movement for Calico Hills. Solid Line - Average Properties; Dotted Line - Limit Properties.

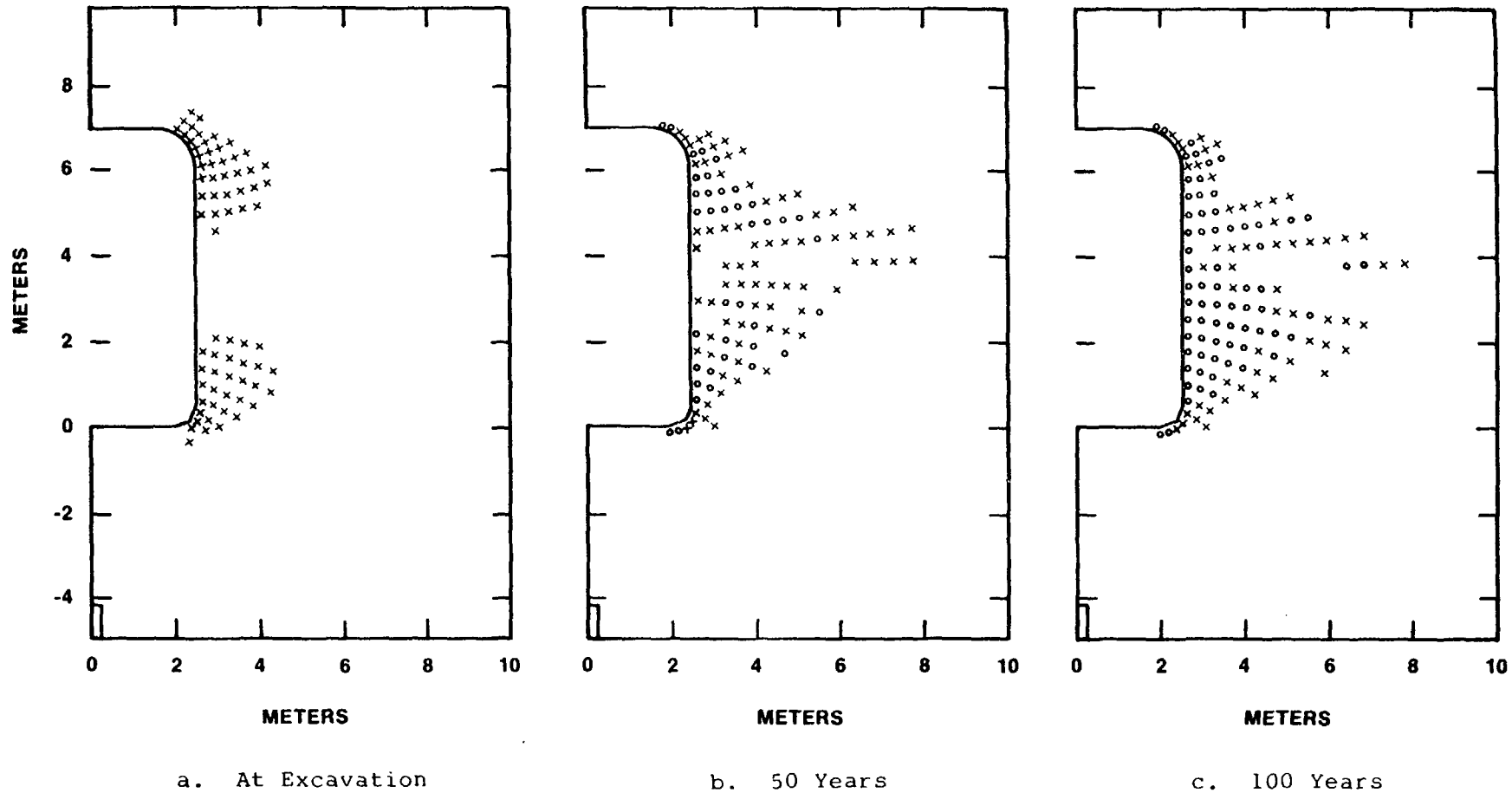
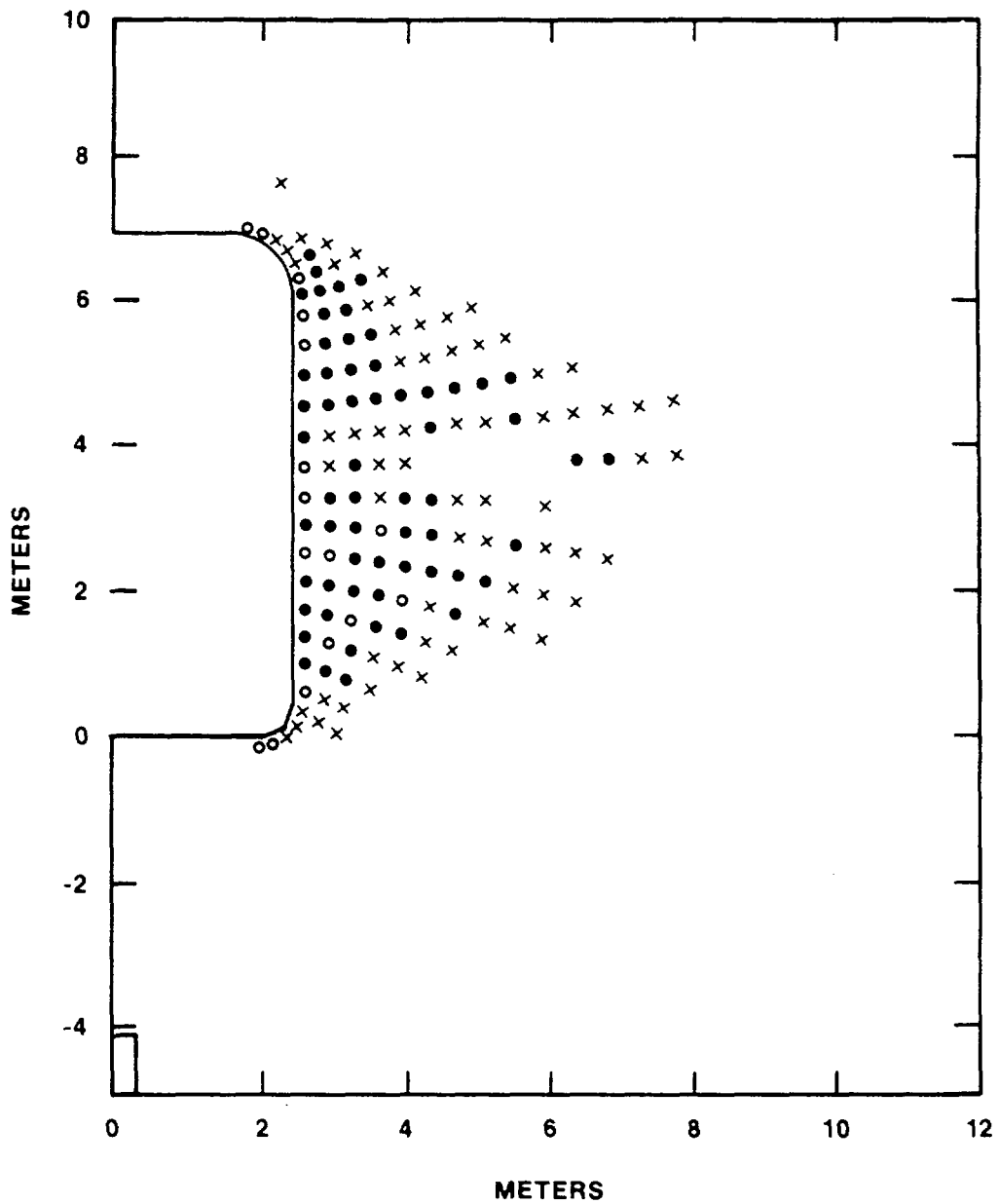
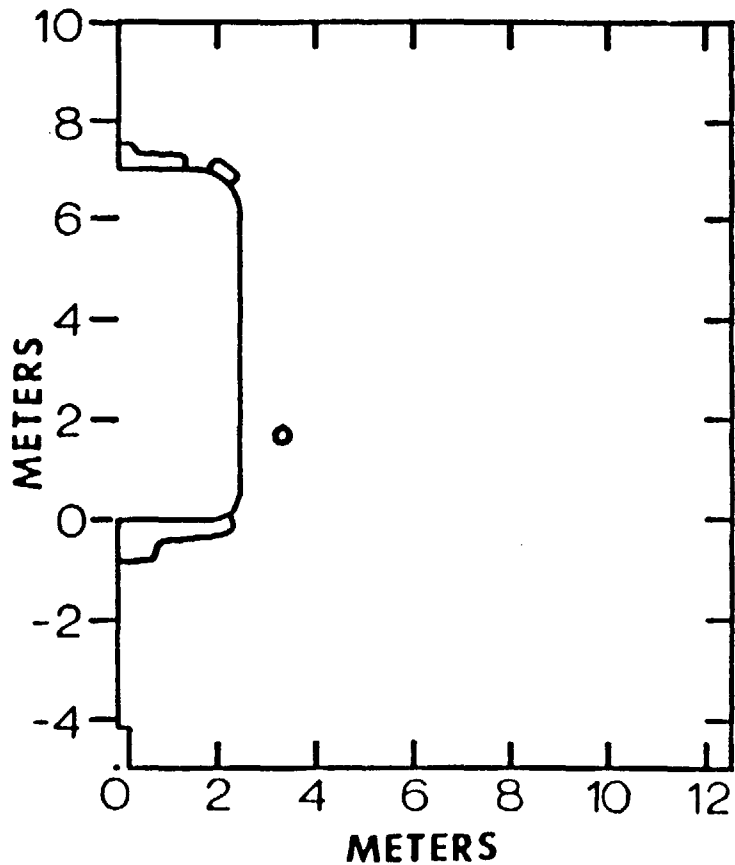


Figure 14. Joint Movement at Various Times for Calico Hills (Limit Properties). x - Joint Closed but Slipping; o - Joint Opening.

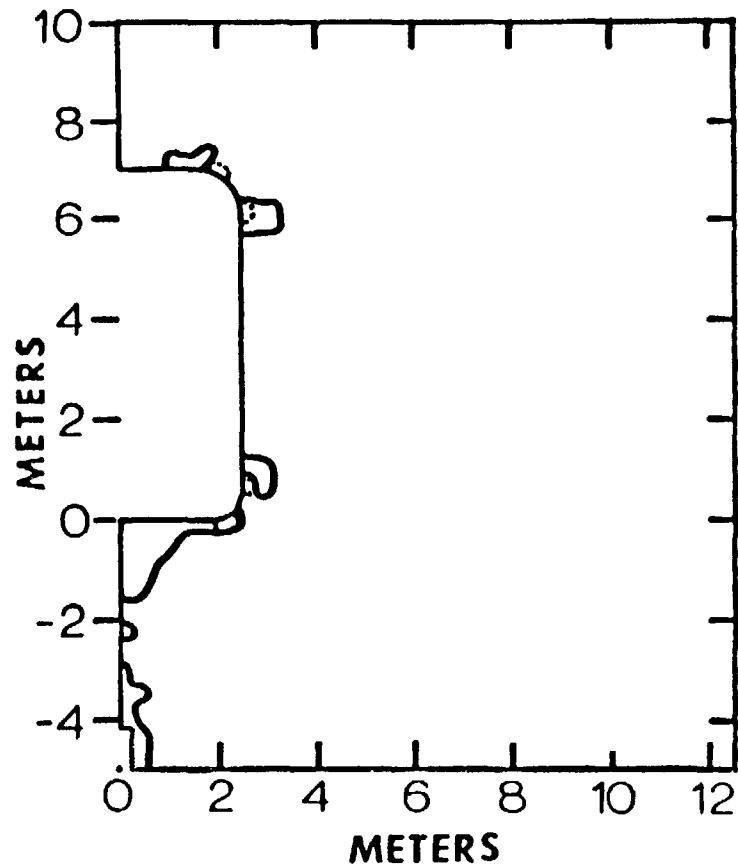


- X - Joint Closed but Slipping
- O - Joint Opening
- - Joint Slipping and Opening

Figure 15. Cumulative Joint Movement in First 100 Years for Calico Hills (Limit Properties).



a. Average Properties



b. Limit Properties

Figure 16. Fractured Matrix Regions for Calico Hills
Due to Excavation (Dotted Line) and 100
Years of Heating (Solid Line)

Only small regions of matrix failure are predicted at the corners of the room, using limit case properties. At 100 years after emplacement, the matrix failure zone predicted using limit case properties extended into the floor and around the waste canister as the result of heating.

Safety factor contours against additional rock matrix failure are shown at excavation and at 50 years and 100 years after emplacement of the waste for average case properties in Figure 17 and for limit case properties in Figure 18.

The Calico Hills is not a highly fractured rock, therefore the ubiquitous joint model may not be an accurate representation of the behavior of this rock. For this reason, the calculations were repeated after deleting the joints from the model. For average case material properties no matrix failure was predicted in the pillars while a similar amount of matrix failure was observed in the floor and roof of the room as for the ubiquitous joint model. Predicted regions of fractured matrix occurring at excavation and at 100 years after emplacement for limit case properties with joints deleted are shown in Figures 19a and 19b, respectively. For this case, the zone of matrix failure extended along the room rib and into the pillar a small distance (approximately 1 meter) which was not observed in the ubiquitous joint modeling. Since joint movement is limited in this case to cracks produced by matrix failure, the zone of joint movement is much smaller than that occurring with ubiquitous jointing.

Grouse Canyon

In an attempt to correlate the results of finite element calculations with observed behavior of existing underground openings, a calculation using the same room and pillar geometry was made using average properties for the welded Grouse Canyon Tuff in G-Tunnel. Room and pillar geometry used in the calculations was the same as for all other horizons. The result of this calculation at excavation of the room is shown in Figure 20. Regions of joint movement are similar to those of the Yucca Mountain units. A comparison of the behavior of all units, including Grouse Canyon, is shown in Figure 21. Note that Calico Hills is the only unit that shows behavior substantially different from the other horizons, including Grouse Canyon.

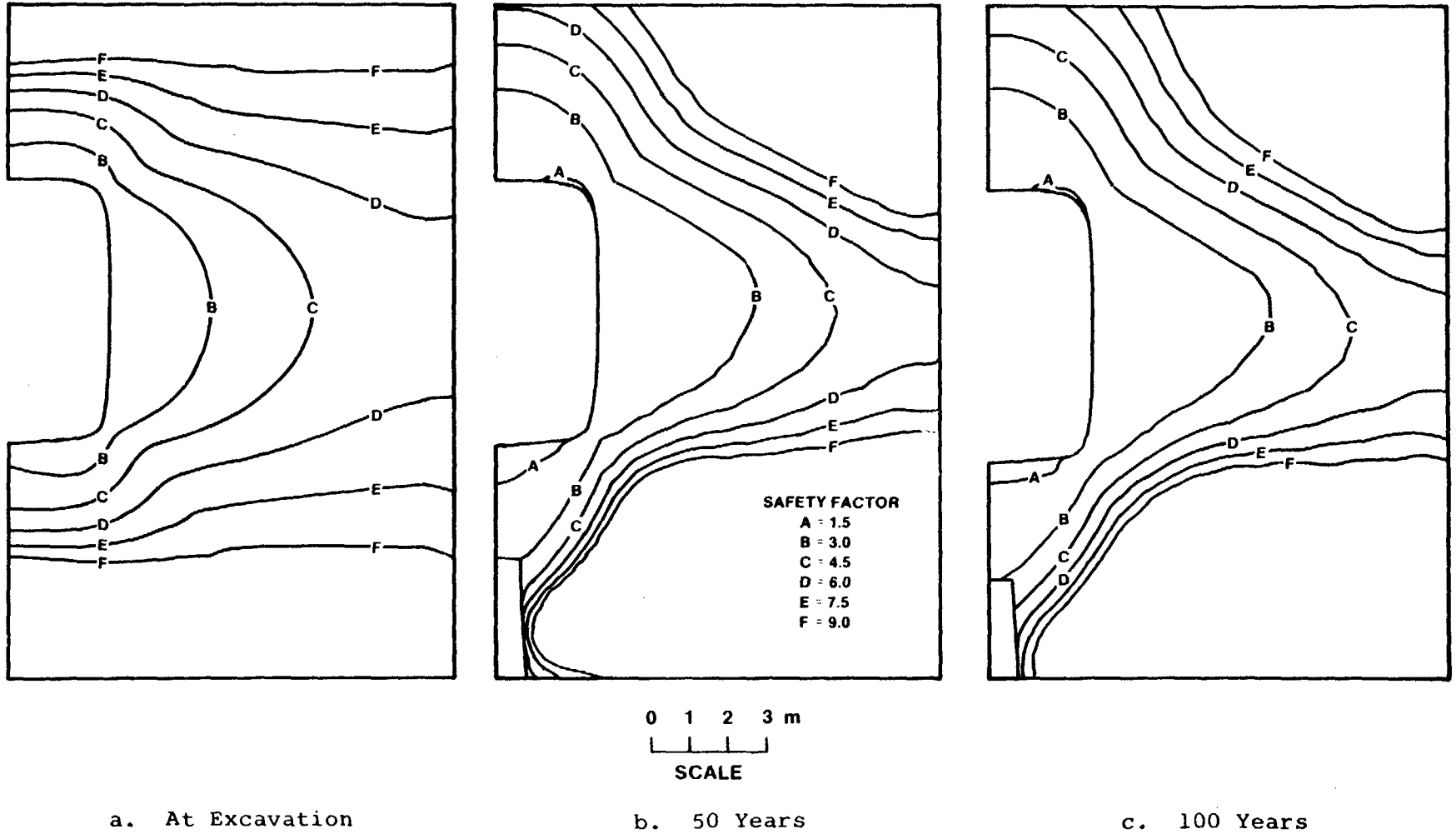
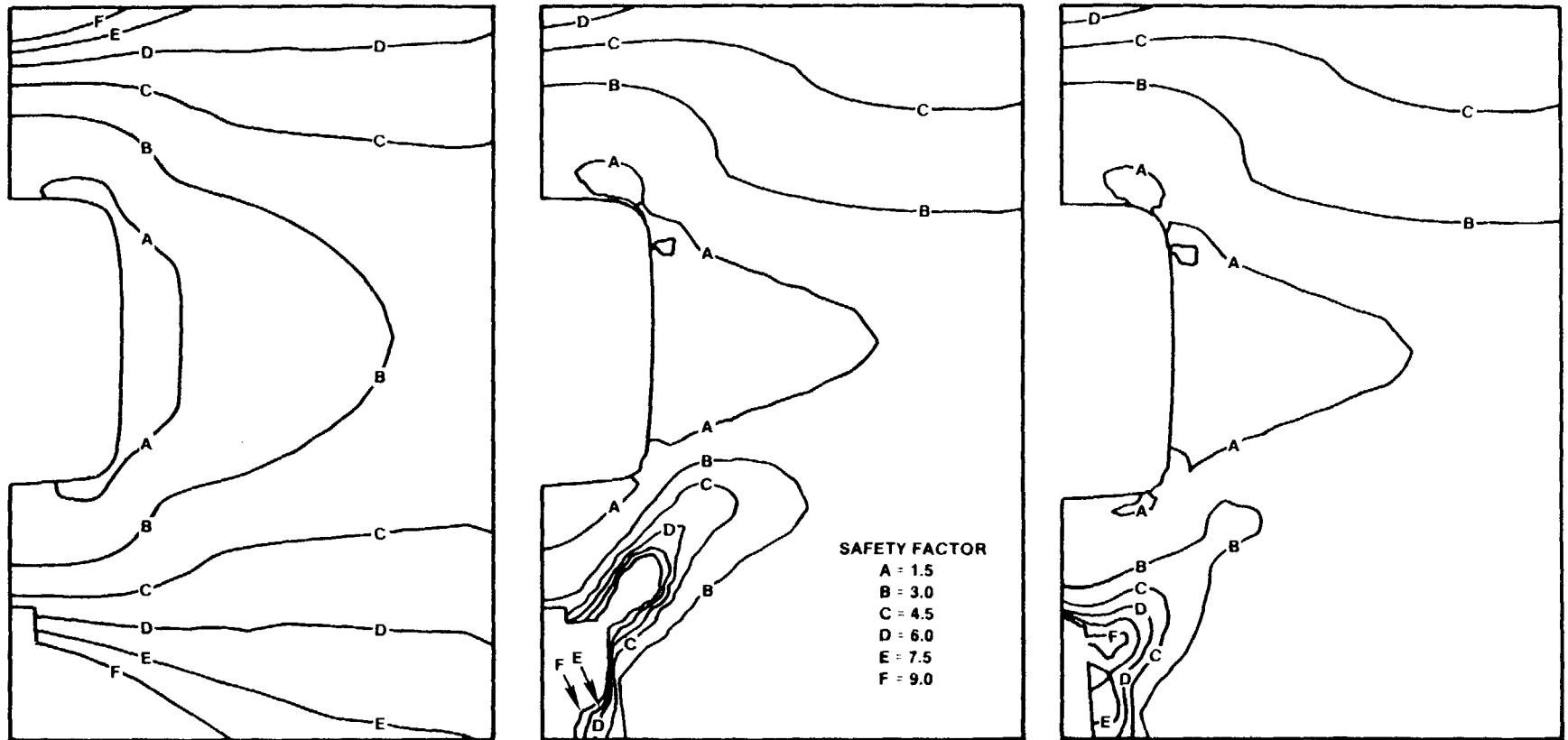


Figure 17. Matrix Factor of Safety Contours for Calico Hills (Average Properties) at Various Times.

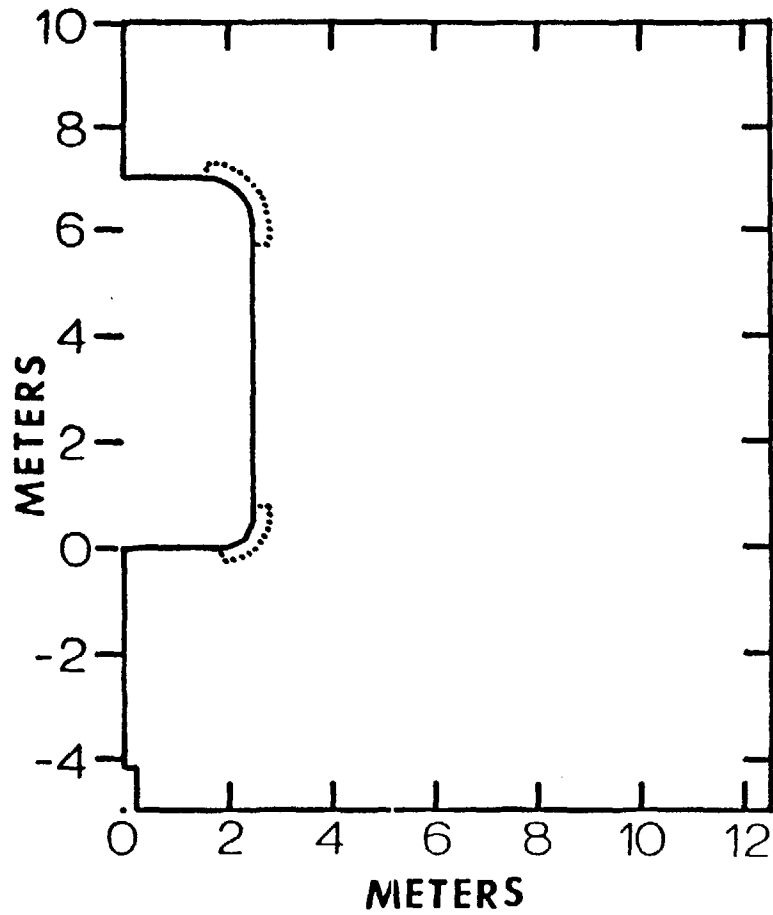


a. At Excavation

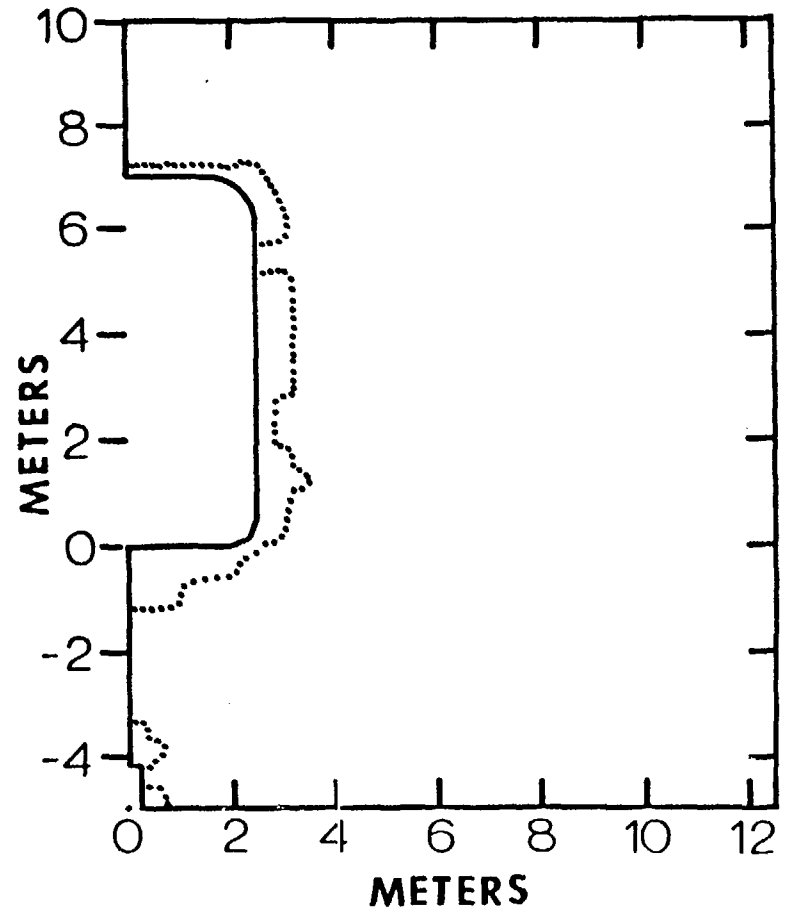
b. 50 Years

c. 100 Years

Figure 18. Matrix Factor of Safety Contours for Calico Hills (Limit Properties) at Various Times.



a. At Excavation



b. 100 Years

Figure 19. Fractured Matrix Regions for Calico Hills (Limit Properties) with Ubiquitous Joints Deleted.

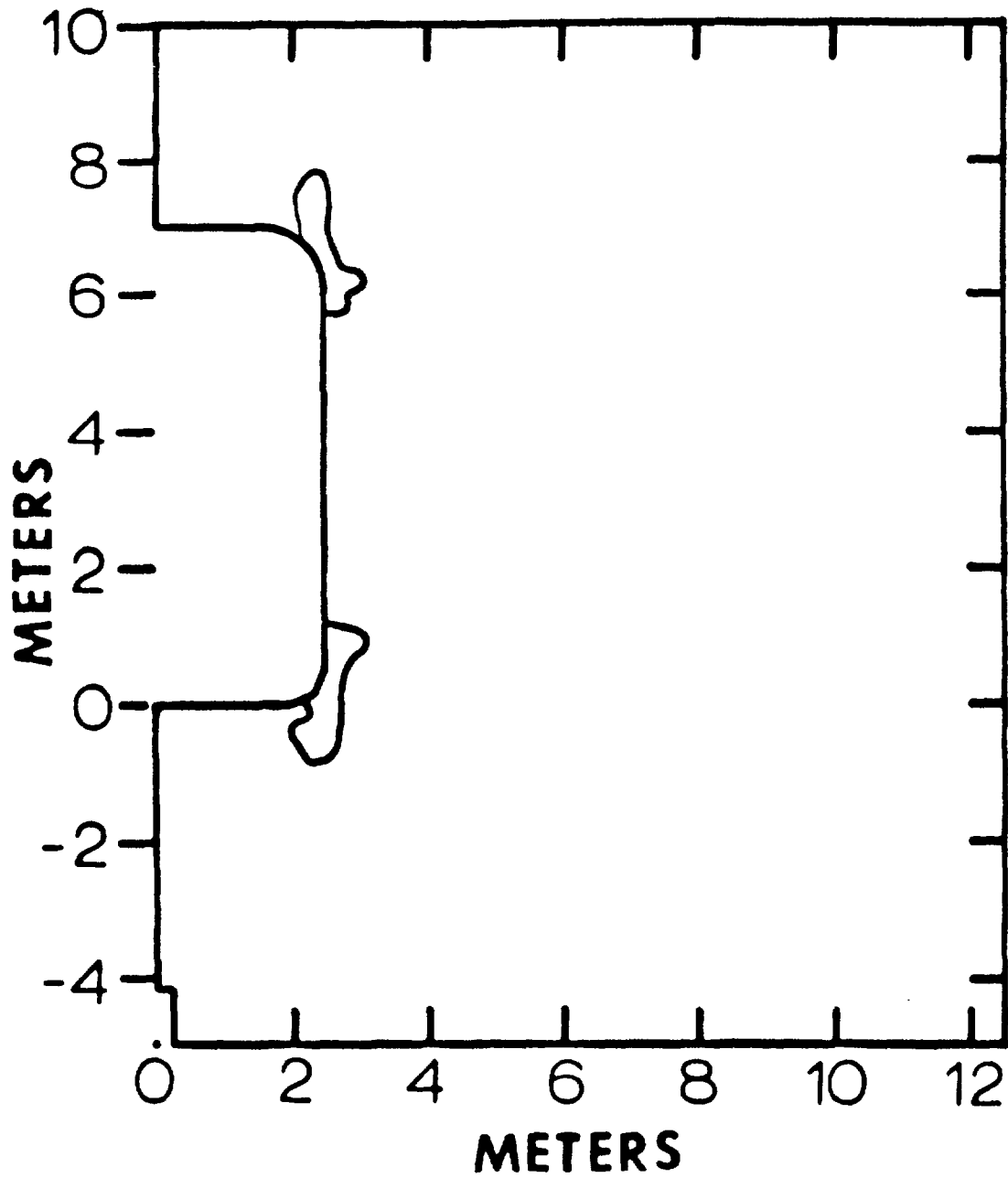


Figure 20. Regions of Joint Movement for Grouse Canyon at Excavation.

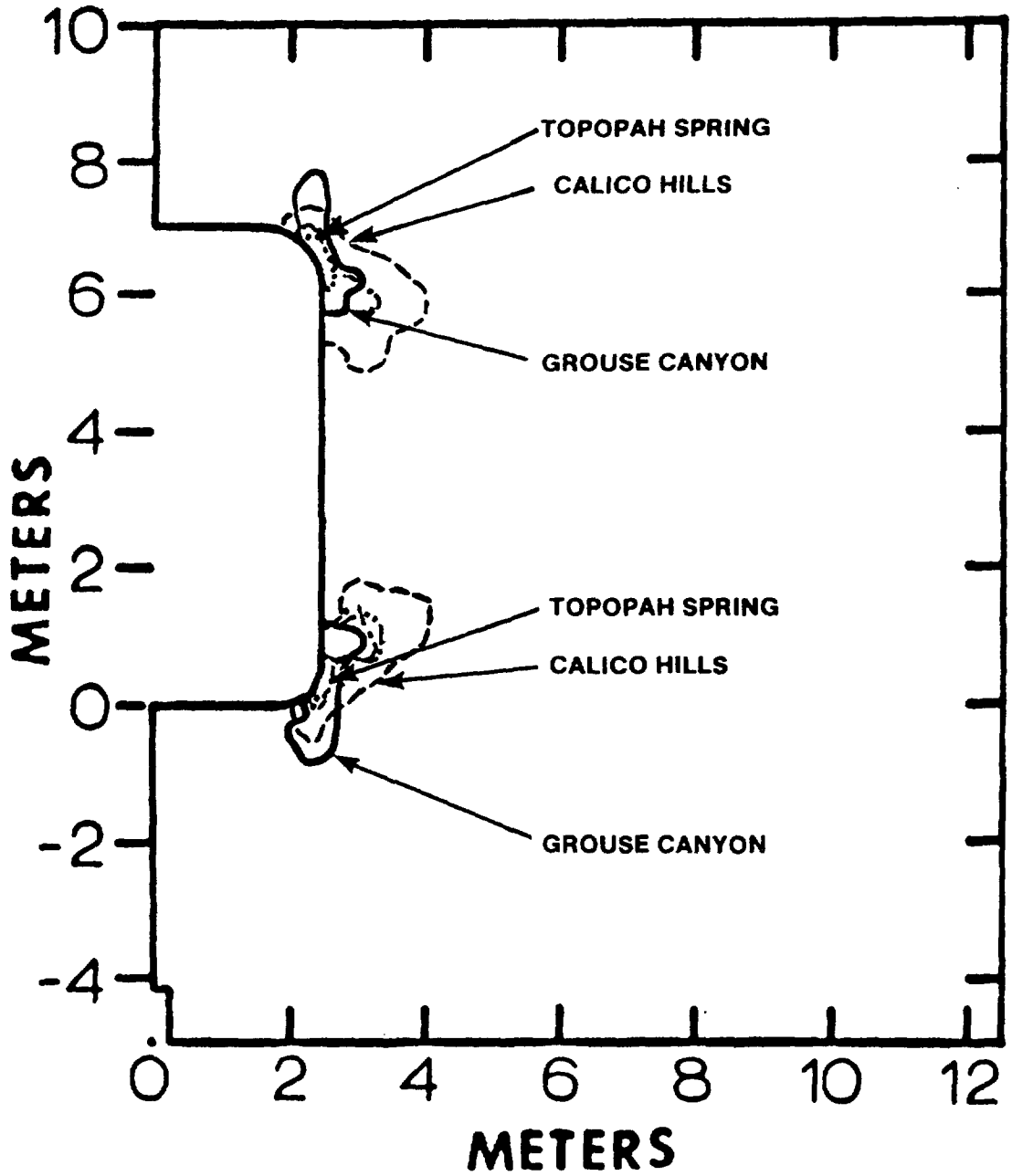


Figure 21. Comparison of Regions of Predicted Joint Movement at Excavation for All Horizons Including Grouse Canyon.

Examination of the corners of the rooms in the Grouse Canyon that have been open for 6 years or more have shown no evidence of preferential rock falls. In fact, completely unsupported spans of drifts up to 30 feet in length have stood for periods of a week or more during drilling and blasting operations with no evidence of rock fall at the corners or in any other part of the room.

Discussion

It should be noted that joint movement predicted by the ubiquitous jointed rock model is based on infinitesimal strain theory. Extension of this theory to the prediction of gross joint movement, including the potential for rockfall, is not possible, except by engineering judgment. Furthermore, no attempt is made to account for motion inhibition effects of intersecting joints and the subsequent interferences that would be expected with the blocky nature of the rock mass. Consequently, the analyses reported here, most likely, overpredict the potential for real joint motion in the field. By comparing the results of calculations for Calico Hills with and without jointing, it can be surmised that joint slip is a stress relieving mechanism in that no matrix failure occurs at excavation when joints are present. Conversely, when joints are removed, matrix failure occurs in both the upper and lower corners of the room at excavation. The matrix failures predicted at excavation are minor in that they are limited to the first row of integration points near the surface of the drift.

What can be derived from the series of calculations just described is information regarding relative behavior that can then be used to compare and contrast the predicted behavior of the units that have different material properties.

A comparison of regions of joint movement for the two welded unit regions shows that they are very similar in size and shape and lie within the influence of standard rockbolt and wire mesh support procedures. Very little rock matrix failure was predicted for the welded units; it was all confined to within less than a meter of the free surface. Regions of joint movement in the Calico Hills are larger in extent than in the welded units, with a tendency of the joints to open later in time due to thermal loading, particularly between 50 and 100 years after emplacement of the waste. This is due primarily to the negative coefficients of thermal expansion of the

Calico Hills. Upon heating the unit contracted locally. Removal of the ubiquitous jointing for Calico Hills produced no additional rock matrix failure for average material properties. With limit properties and no jointing, some additional rock matrix failure was predicted along the room rib and extending a small distance into the pillar.

Increased joint opening was exhibited by both units between 50 and 100 years after emplacement of the waste. For the material model used, this results in a complete loss in shear stiffness in the plane of the joint.

A distinction can be made between the welded Topopah Spring and the nonwelded Calico Hills based upon predicted regions of joint movement. For both average and limit cases, there appears to be more joint movement predicted for the Calico Hills unit than the Topopah Spring unit at any given time. This is especially apparent in view of the tendency toward joint opening later in time.

Another comparison of the performance of the units is provided by an examination of safety factors against rock matrix failure. Limit case safety factors are found to be lower than average case values when the contours are compared. One reason for this is the reduction in rock strength when going from average to limit case values (ranging from 7% to 37% of average case values). There is also a trend toward lower factors of safety with increasing depth due to the increase in overburden stress.

For excavation-induced loads, Topopah Spring appears to deform least, as interpreted through examining the safety factor contours. This makes sense in that it is the shallowest and stiffest unit. It should be noted that only the Calico Hills limit case showed safety factor contours as low as 1.5, and only the Calico Hills showed matrix failure at the corners of the room for average properties. In all other cases, the lowest safety factor observed was 3. The safety factor predicted for the Topopah Spring is clearly the most favorable. The regions of deformation (as interpreted through examining the safety factor contours) predicted in the Calico Hills appears minor, well within standard support technology.

At 50 years after emplacement of the waste, both units remain stable when average case properties are used, but again Calico Hills has the lowest safety factors against rock matrix failure. Comparison of the 50-year limit case contours shows that the Topopah Spring unit exhibits a decrease in the safety factor in the room floor and roof while maintaining the safety

factors in the pillar. The Calico Hills exhibits safety factors of less than 1.5 (but greater than 1) at the rib and extending into the pillar.

Deformation due to joint movement and/or rock matrix failure is perhaps no more extensive than would be expected from drilling and blasting mining effects [21].

The comparison of the behavior of the Topopah Spring and Calico Hills units with the observed and predicted behavior of similar excavations in G-Tunnel would indicate that finite element code prediction of joint movement does not necessarily correlate with room instability.

SUMMARY AND CONCLUSIONS

Summary

Calculations have been completed for the Topopah Spring and Calico Hills units using average and limit case material properties. Maximum GTLs have been determined for each of the horizons based on maintaining a maximum floor temperature of 100 C at 110 years after emplacement of the waste.

Other calculations using average properties of the Grouse Canyon Tuff in G-Tunnel were also done to compare the performance at excavation of the Topopah Spring and Calico Hills units with that of a geological unit of known performance.

Suitability of all horizons as potential candidates for a repository were evaluated by comparing (1) capacity for waste storage based on maximum or optimized GTL, (2) regions of predicted joint slip as the result of excavation and subsequent thermal loading, (3) regions of predicted rock matrix failure as the result of excavation and subsequent thermal loading, and (4) safety factors against rock matrix failure.

Concerns addressed were (1) stability of the room and pillar subsequent to excavation, and (2) stability of the room and pillar after emplacement of the waste and subsequent heating to the 100 year time frame.

Sufficient data were obtained from this series of calculations using an identical thermomechanical model to make comparisons of the units in terms of waste storage capacity and room and pillar stability.

Conclusions

Performance of the horizons was assessed on the basis of three different criteria: (1) capacity for waste storage, (2) the ability to excavate an opening, and (3) long-term stability of the excavated room during an extended period of heating for up to 100 years after waste emplacement.

Based on waste storage capacity as determined through the concept of maximum GTL [2], the Topopah Spring is the first choice followed by the Bullfrog and Tram units, and lastly by the Calico Hills. The total difference in the maximum GTL is small, from the highest to the lowest is only 3 kW/acre.

The ability to produce a stable excavated opening again shows the Topopah Spring unit to be equal to or better than the other units.

Long-term stability of the excavated rooms, as determined by evaluating regions of predicted joint slip as the result of excavation and subsequent thermal loading, evaluating regions of predicted rock matrix failure as the result of excavation and subsequent thermal loading, and evaluating safety factors against rock matrix failure, implied that the the Topopah Spring is the first choice, followed by the Bullfrog, Tram, and Calico Hills.

In this study, opening stability through a time period of 100 years (as evaluated by examining the thermal induced load through time) was assessed for four units at Yucca Mountain. The units possess a wide range of material properties and are located at various depths (thus in situ stresses vary). For all of these variations in material properties and in situ stresses considered, the predictions are of stable openings. It is prudent to further conclude that future calculations would predict stable openings if the material properties used, and in situ stresses fell within the ranges considered here.

It is important to note that the results of the thermal and mechanical calculations did not eliminate any of the horizons on the basis of unacceptable behavior. In all cases the calculated regions of damage in the vicinity of the room and pillar were well within the limits of existing support capabilities, and no more than might be observed for standard drill and blast mining effects. In all cases the Topopah Spring unit was equal to

or better than the other units. Criteria other than that presented here was used to recommend the Topopah Spring unit [2].

REFERENCES

1. Thomas, R. K., "NNWSI Unit Evaluation at Yucca Mountain, Nevada Test Site: Near Field Mechanical Calculations Using a Continuum Jointed Rock Model in the JAC Code," SAND83-0070, Sandia National Laboratories, Albuquerque NM, 1987.
2. Johnstone, J. K., Peters, R. R., and Gnirk, P. F., "Unit Evaluation at Yucca Mountain, Nevada Test Site: Summary Report and Recommendations," SAND83-0372, Sandia National Laboratories, Albuquerque NM, June 1984.
3. Peters, R. R. and Lappin, A. R., Sandia National Laboratories, to Brandshaug, T., RE/SPEC Inc., "Revised Far-Field Thermomechanical Calculations for Four Average Property Cases," Memorandum dtd August 17, 1982.
4. Peters, R. R. and Lappin, A. R., Sandia National Laboratories, to Brandshaug, T., RE/SPEC Inc., "Revised Far Field Thermomechanical alculations for Four "Limit" Property Cases," Memorandum dtd September 22, 1982.
5. Peters, R. R., to Thomas, R. K., Sandia National Laboratories, "Thermomechanical Calculations for Unit Evaluation," Memorandum dtd October 25, 1982.
6. Peters, R. R., Sandia National Laboratories, to Key, S. W., RE/SPEC Inc., "Thermomechanical Calculations for Unit Evaluation," Memorandum dtd October 25, 1982.
7. Peters, R. R., to Krieg, R. D., Sandia National Laboratories, "Near Field Thermomechanical Calculations in the Welded, Devitrified Portion of the Grouse Canyon Member of the Belted Range Tuff (G-Tunnel Tuff)," Memorandum dtd November 29, 1982.
8. Price, R. H., "Analysis of Rock Mechanics Properties of Volcanic Tuff Units from Yucca Mountain, Nevada Test Site," SAND82-1315, Sandia National Laboratories, Albuquerque NM, August 1983.
9. Lappin, A. R., Sandia National Laboratories, to Distribution, "Bulk and Thermal Properties of the Functional "Tuffaceous Beds," Here Defined to Include the Basal Topopah Spring, All of the Tuffaceous Beds of Calico Hills, and the Upper Portion of the Prow Pass," Memorandum dtd March 26, 1982.
10. Lappin, A. R., Sandia National Laboratories, to Distribution, "Bulk and Thermal Properties for the Welded, Devitrified Portions of the Bullfrog and Tram Members, Crater Flat Tuff," Memorandum dtd April 19, 1982.
11. Lappin, A. R., Sandia National Laboratories, to Distribution, "Bulk and Thermal Properties of the Potential Emplacement Horizon Within the Densely Welded, Devitrified Portion of the Topopah Spring Member of the Paintbrush Tuff," Memorandum dtd June 30, 1982.

12. Bathe, Klaus-Jurgen, "ADINAT: A Finite Element Program for Automatic Dynamic Incremental Nonlinear Analysis of Temperatures," Report 82448-5, Massachusetts Institute of Technology, May, 1977 (Rev. Dec. 1978).
13. Thomas, R. K., "A Material Constitutive Model for Jointed Rock Mass Behavior," SAND80-1418, Sandia National Laboratories, Albuquerque NM, November 1980.
14. Johnson, R. L. and Thomas, R. K., "A Constitutive Model for Ubiquitously Jointed Rock Masses," Proceedings International Conference on Constitutive Laws for Engineering Materials: "Theory and Application," Tuscon, Arizona, January, 1983.
15. Bathe, Klaus-Jurgen, "ADINA: A Finite Element Program for Automatic Dynamic Incremental Nonlinear Analysis," Report 82448-1, Massachusetts Institute of Technology, September, 1975 (Rev. Dec. 1978).
16. Flanagan, Dennis P., "DETOUR-A Deformed Mesh/Contour Plotting Program: Preliminary Users Guide."
17. Johnson, Roy L., "Thermomechanical Scoping Calculations for a High-Level Nuclear Waste Repository in Tuff," SAND81-0629, Albuquerque, Sandia National Laboratories, June, 1981.
18. Johnson, Roy L. and Flanagan, Dennis P., "Effects of the Variation of Material Properties on the Performance of a Nuclear Waste Repository Sited in Welded Tuff," SAND83-1679, Albuquerque, Sandia National Laboratories, in preparation.
19. Gartling, David K., Eaton, Roger P., and Thomas, Robert K., "Preliminary Thermal Analysis for a Nuclear Waste Repository in Tuff," SAND80-2813, Sandia National Laboratories, Albuquerque NM, April 1981.
20. Gartling, David K., "MERLIN-A Computer Program to Transfer Data Between Finite Element Meshes," SAND81-0463, Sandia National Laboratories, Albuquerque NM, September, 1981.
21. Hustrulid, W. A., Colorado School of Mines, to J. K. Johnstone, Sandia National Laboratories, Personal Communication, January 25, 1983.

Appendix I

RIB and SEPDB Data Appendix

No RIB or SEPDB data were used in this report as the work predates the existence of both the RIB and SEPDB. Thermal and thermomechanical properties of the units in Yucca Mountain were used extensively in this report. These properties (limit and average) were defined in support of the unit evaluation study [2]. The average properties are in general agreement with the equivalent properties currently in the RIB since the RIB values were developed based upon much of the same data (and with additions in many areas) used to support the unit evaluation effort.

DISTRIBUTION LIST

B. C. Rusche (RW-1)
Director
Office of Civilian Radioactive
Waste Management
U.S. Department of Energy
Forrestal Building
Washington, DC 20585

Ralph Stein (RW-23)
Office of Civilian Radioactive
Waste Management
U.S. Department of Energy
Forrestal Building
Washington, DC 20585

J. J. Fiore, (RW-221)
Office of Civilian Radioactive
Waste Management
U.S. Department of Energy
Forrestal Building
Washington, DC 20585

M. W. Frei (RW-231)
Office of Civilian Radioactive
Waste Management
U.S. Department of Energy
Forrestal Building
Washington, DC 20585

E. S. Burton (RW-25)
Siting Division
Office of Geologic Repositories
U.S. Department of Energy
Forrestal Building
Washington, D.C. 20585

C. R. Cooley (RW-24)
Geosciences & Technology Division
Office of Geologic Repositories
U.S. Department of Energy
Forrestal Building
Washington, DC 20585

V. J. Cassella (RW-222)
Office of Civilian Radioactive
Waste Management
U.S. Department of Energy
Forrestal Building
Washington, DC 20585

T. P. Longo (RW-25)
Program Management Division
Office of Geologic Repositories
U.S. Department of Energy
Forrestal Building
Washington, DC 20585

Cy Klingsberg (RW-24)
Geosciences and Technology Division
Office of Geologic Repositories
U. S. Department of Energy
Forrestal Building
Washington, DC 20585

B. G. Gale (RW-223)
Office of Civilian Radioactive
Waste Management
U.S. Department of Energy
Forrestal Building
Washington, DC 20585

R. J. Blaney (RW-22)
Program Management Division
Office of Geologic Repositories
U.S. Department of Energy
Forrestal Building
Washington, DC 20585

R. W. Gale (RW-40)
Office of Civilian Radioactive
Waste Management
U.S. Department of Energy
Forrestal Building
Washington, D.C. 20585

J. E. Shaheen (RW-44)
Outreach Programs
Office of Policy, Integration and
Outreach
U.S. Department of Energy
Forrestal Building
Washington, DC 20585

J. O. Neff, Manager
Salt Repository Project Office
U.S. Department of Energy
505 King Avenue
Columbus, OH 43201

D. C. Newton (RW-23)
Engineering & Licensing Division
Office of Geologic Repositories
U.S. Department of Energy
Forrestal Building
Washington, DC 20585

S. A. Mann, Manager
Crystalline Rock Project Office
U.S. Department of Energy
9800 South Cass Avenue
Argonne, IL 60439

O. L. Olson, Manager
Basalt Waste Isolation Project Office
Richland Operations Office
U.S. Department of Energy
Post Office Box 550
Richland, WA 99352

K. Street, Jr.
Lawrence Livermore National
Laboratory
Post Office Box 808
Mail Stop L-209
Livermore, CA 94550

D. L. Vieth, Director (4)
Waste Management Project Office
U.S. Department of Energy
Post Office Box 14100
Las Vegas, NV 89114

L. D. Ramspott (3)
Technical Project Officer for NNWSI
Lawrence Livermore National
Laboratory
P.O. Box 808
Mail Stop L-204
Livermore, CA 94550

D. F. Miller, Director
Office of Public Affairs
U.S. Department of Energy
Post Office Box 14100
U.S. Department of Energy
Las Vegas, NV 89114

W. J. Purcell (RW-20)
Associate Director
Office of Civilian Radioactive
Waste Management
U.S. Department of Energy
Forrestal Building
Washington, DC 20585

P. M. Bodin (12)
Office of Public Affairs
U.S. Department of Energy
Post Office Box 14100
Las Vegas, NV 89114

D. T. Oakley (4)
Technical Project Officer for NNWSI
Los Alamos National Laboratory
P.O. Box 1663
Mail Stop F-619
Los Alamos, NM 87545

B. W. Church, Director
Health Physics Division
U.S. Department of Energy
Post Office Box 14100
Las Vegas, NV 89114

L. R. Hayes (3)
Technical Project Officer for NNWSI
U.S. Geological Survey
Post Office Box 25046
421 Federal Center
Denver, CO 80225

Chief, Repository Projects Branch
Division of Waste Management
U.S. Nuclear Regulatory Commission
Washington, D.C. 20555

NTS Section Leader
Repository Project Branch
Division of Waste Management
U.S. Nuclear Regulatory Commission
Washington, D.C. 20555

Document Control Center
Division of Waste Management
U.S. Nuclear Regulatory Commission
Washington, D.C. 20555

V. M. Glanzman
U.S. Geological Survey
Post Office Box 25046
913 Federal Center
Denver, CO 80225

P. T. Prestholt
NRC Site Representative
1050 East Flamingo Road
Suite 319
Las Vegas, NV 89109

M. E. Spaeth
Technical Project Officer for NNWSI
Science Applications
International Corporation
Suite 407
101 Convention Center Drive
Las Vegas, NV 89109

SAIC-T&MSS Library (2)
Science Applications
International Corporation
Suite 407
101 Convention Center Drive
Las Vegas, NV 89109

W. S. Twenhofel, Consultant
Science Applications
International Corp.
820 Estes Street
Lakewood, CO 89215

A. E. Gurrola
General Manager
Energy Support Division
Holmes & Narver, Inc.
Mail Stop 580
Post Office Box 14340
Las Vegas, NV 89114

J. A. Cross, Manager
Las Vegas Branch
Fenix & Scisson, Inc.
Mail Stop 514
Post Office Box 14308
Las Vegas, NV 89114

Neal Duncan (RW-44)
Office of Policy, Integration, and
Outreach
U.S. Department of Energy
Forrestal Building
Washington, DC 20585

J. S. Wright
Technical Project Officer for NNWSI
Westinghouse Electric Corporation
Waste Technology Services Division
Nevada Operations
Post Office Box 708
Mail Stop 703
Mercury, NV 89023

ONWI Library
Battelle Columbus Laboratory
Office of Nuclear Waste Isolation
505 King Avenue
Columbus, OH 43201

W. M. Hewitt, Program Manager
Roy F. Weston, Inc.
955 L'Enfant Plaza, Southwest, Suite 800
Washington, DC 20024

H. D. Cunningham
General Manager
Reynolds Electrical &
Engineering Co., Inc.
Post Office Box 14400
Mail Stop 555
Las Vegas, NV 89114

T. Hay, Executive Assistant
Office of the Governor
State of Nevada
Capitol Complex
Carson City, NV 89710

R. R. Loux, Jr., Executive Director (3)
Nuclear Waste Project Office
State of Nevada
Evergreen Center, Suite 252
1802 North Carson Street
Carson City, NV 89701

C. H. Johnson, Technical
Program Manager
Nuclear Waste Project Office
State of Nevada
Evergreen Center, Suite 252
1802 North Carson Street
Carson City, NV 89701

John Fordham
Desert Research Institute
Water Resources Center
Post Office Box 60220
Reno, NV 89506

Department of Comprehensive
Planning
Clark County
225 Bridger Avenue, 7th Floor
Las Vegas, NV 89155

Lincoln County Commission
Lincoln County
Post Office Box 90
Pioche, NV 89043

Community Planning and
Development
City of North Las Vegas
Post Office Box 4086
North Las Vegas, NV 89030

City Manager
City of Henderson
Henderson, NV 89015

N. A. Norman
Project Manager
Bechtel National Inc.
P. O. Box 3965
San Francisco, CA 94119

Flo Butler
Los Alamos Technical Associates
1650 Trinity Drive
Los Alamos, New Mexico 87544

Timothy G. Barbour
Science Applications
International Corporation
1626 Cole Boulevard, Suite 270
Golden, CO 80401

E. P. Binnall
Field Systems Group Leader
Building 50B/4235
Lawrence Berkeley Laboratory
Berkeley, CA 94720

Dr. Martin Mifflin
Desert Research Institute
Water Resources Center
Suite 1
2505 Chandler Avenue
Las Vegas, NV 89120

Planning Department
Nye County
Post Office Box 153
Tonopah, NV 89049

Economic Development
Department
City of Las Vegas
400 East Stewart Avenue
Las Vegas, NV 89101

Director of Community
Planning
City of Boulder City
Post Office Box 367
Boulder City, NV 89005

Commission of the
European Communities
200 Rue de la Loi
B-1049 Brussels
BELGIUM

Technical Information Center
Roy F. Weston, Inc.
955 L'Enfant Plaza, Southwest, Suite 800
Washington, DC 20024

R. Harig
Parsons Brinkerhoff Quade &
Douglas, Inc.
1625 Van Ness Ave.
San Francisco, CA 94109-3678

Dr. Madan M. Singh, President
Engineers International, Inc.
98 East Naperville Road
Westmont, IL 60559-1595

Roger Hart
Itasca Consulting Group, Inc.
P.O. Box 14806
Minneapolis, Minnesota 55414

T. H. Isaacs (RW-22)
Office of Civilian Radioactive
Waste Management
U.S. Department of Energy
Forrestal Building
Washington, DC 20585

J. P. Knight (RW-24)
Office of Civilian Radioactive
Waste Management
U.S. Department of Energy
Forrestal Building
Washington, DC 20585

D. H. Alexander (RW-232)
Office of Civilian Radioactive
Waste Management
U.S. Department of Energy
Forrestal Building
Washington, DC 20585

Allen Jelacic (RW-233)
Office of Civilian Radioactive
Waste Management
U.S. Department of Energy
Forrestal Building
Washington, DC 20585

B. J. King, Librarian (2)
Basalt Waste Isolation Project
Library
Rockwell Hanford Operations
Post Office Box 800
Richland, WA 99352

J. R. Rollo
Deputy Assistant Director
for Engineering Geology
U.S. Geological Survey
106 National Center
12201 Sunrise Valley Drive
Reston, VA 22092

David K. Parrish
RE/SPEC Inc.
3815 Eubank, N.E.
Albuquerque, NM 87191

R. Lindsay Mundell
United States Bureau of Mines
P.O. Box 25086
Building 20
Denver Federal Center
Denver, Colorado 80225

D. L. Fraser, General Manager
Reynolds Electrical & Engineering
Co., Inc.
Mail Stop 555
Post Office Box 14400
Las Vegas, NV 89114-4400

Vincent Gong
Technical Project Officer for NNWSI
Reynolds Electrical & Engineering
Co., Inc.
Mail Stop 615
Post Office Box 14400
Las Vegas, NV 89114-4400

Gerald Parker (RW-241)
Office of Civilian Radioactive
Waste Management
U.S. Department of Energy
Forrestal Building
Washington, DC 20585

Christopher M. St. John
J. F. T. Agapito Associates, Inc.
27520 Hawthorne Blvd., Suite 137
Rolling Hills Estates, CA 90274

J. P. Pedalino
Technical Project Officer for NNWSI
Holmes & Narver, Inc.
Mail Stop 605
Post Office Box 14340
Las Vegas, NV 89114

S. D. Murphy
Technical Project Officer for NNWSI
Fenix & Scisson, Inc.
Mail Stop 514
Post Office Box 15408
Las Vegas, NV 89114

Eric Anderson
Mountain West Research-Southwest, Inc.
398 South Mill Avenue, Suite 300
Tempe, AZ 85281

S. H. Kale (RW-20)
Office of Civilian Radioactive
Waste Management
U.S. Department of Energy
Forrestal Building
Washington, DC 20585

Judy Foremaster (5)
City of Caliente
Post Office Box 158
Caliente, NV 89008

J. H. Anttonen, Deputy Assistant
Manager for Commercial
Nuclear Waste
Basalt Waste Isolation Project
Office
U.S. Department of Energy
P.O. Box 550
Richland, WA 99352

1523 J. Biffle
1523 R. Johnson (5)
1523 J. Holland
1523 E. P. Chen
5171 R. K. Thomas
6300 R. W. Lynch
6310 T. O. Hunter
6310 71/124211/0/Q3
6311 A. L. Stevens
6311 C. Mora
6311 V. Hinkel (2)
6312 F. W. Bingham
6312 B. S. Langkopf
6313 T. E. Blejwas
6314 J. R. Tillerson
6314 S. J. Bauer (5)
6314 L. S. Costin
6314 B. L. Ehgartner
6314 A. J. Mansure
6315 S. Sinnock
6316 R. B. Pope
6332 WMT Library (20)
6410 N. R. Ortiz
3141 S. A. Landenberger (5)
3151 W. L. Garner (3)
8024 P. W. Dean
3154-3 C. H. Dalin (28)
for DOE/OSTI